Central-Asian Institute for Applied Geosciences

Report

**by results for 2016-17 years
under project: "Ecosystem-based adaptation to climate
change in high mountainous areas of Central Asia"**

**Executors: Usubaliev R., Osmonov A., Mandychev A., Shabunin A.,
Kalashnikova O., Azisov E., Esenaman M., Podrezova J..**

CAIAG

2018

Contents

1. *Pilot site 1*. Kyrgyzstan, Naryn oblast, At-Bashi district, Bash-Kaindy village.

1.1 Results of field work - 2016 - 2017

1. Meteorological research

In October 2016, a field expedition was conducted, where the set-up point for an automatic weather station (AMS) near the village of Bash-Kaindy was determined. On May 30, 2017 the AMS (Fig.1.1, 1.2) was installed at this point, transmitting the main meteorological parameters to the CAIAG through the cellular network. The technical characteristics of the AMS are given in Appendix 1.

Fig. 1.1 Automatic meteorological station near the village of Bash-Kaindy

Fig. 1.2 Geographical location of the AMS near the village of Bash-Kaindy
Coordinates: 75,9425el; 41,1343 nl; height above sea level 2,282 m.

As of the end of 2017, the main meteorological parameters were obtained from the AMS: air temperature, atmospheric precipitation, relative humidity, wind speed and direction. These parameters are accessible via the Internet, through the CAIAG Sensor Data Storage System (SDSS). In order to obtain reliable data on atmospheric precipitation, especially in winter, a Tretyakov precipitation gauge was installed next to the AMS, which was serviced by a local observer. The results of measurements of the main meteorological parameters from the AMS are shown in Figure 1.3.
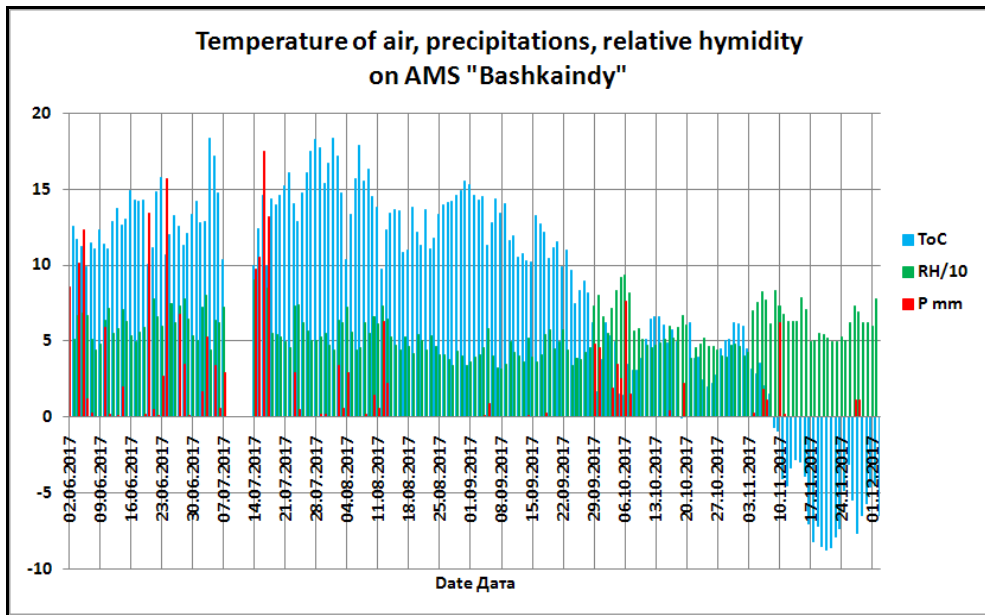
Fig. 1.3 Temperature of surface air, atmospheric precipitation and relative humidity, reduced by 10 times on the Bash-Kaindy AMS

2. Hydrological research

The Bash-Kaindy River is a left tributary of the At-Bashi River, originating from the glaciers of the northern slope of the At-Bashi Ridge, in particular from the No.182 [3] Glacier. In 2017 a hydrological gauging station was set on this river, from the nullah, to the water intake channels; its coordinates are: 75.953217 ° el, 41.125877 ° nl, 2,326 masl. Its location is shown in Figure 1.2 .In the period from April to September 2017, hydrometric measurements of the depth and flow rate were takenevery ten days at this gauging station on the Bash-Kaindy river; the flow velocity was being measured with the GR-21M hydro-metric propeller (velocity flow meter). Then, based on the determination of the river's cross-sectional area, the water discharge was calculated. From April to June and from the second half of August to September, the runoff was monitored at this main gauging station (Fig. 2.1); and in July and early August - at a different, hard-to reach for the observer location,from the bridge upstream (Figure 2.2), since the high water level did not allow to conduct observations at the same location. To conduct instrumental observations, an employee of the Kyrgyzhydromet, a hydro meteorologist with many years' experience of work on the rivers of the Naryn Basin, Imanbaev A.Sh. was involved.
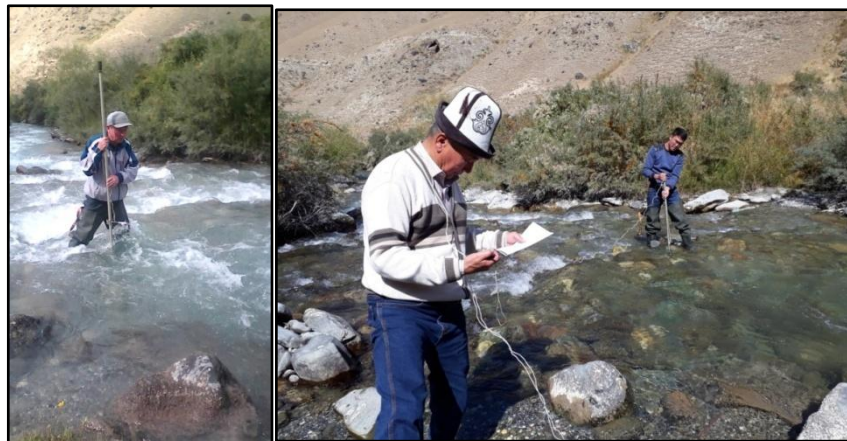
Fig. 2.1 Measurement of the depth and flow rate at the main gauging station on the Bash-Kaindy River on August 17 (left) and September 20 (right).

Fig.2.2 Measurement of the depth and flow velocity in July, upstream from the main gauging station, from the bridge on the Bash-Kaindy River.

The results of runoff monitoring on the Bash-Kaindy River in 2017 are as follows:

- The average runoff during vegetation period - 4.81 m^3/s;
- The maximum water discharge was observed on July 10 - 15.3 m^3/s;
- The minimum water flow was observed on April 20 - 0.21 m^3/s.
The maximum depth of the river was 1.4m, the largest sectional area of the river was 11.6m^2 and the maximum water discharge were observed on July 10. In April, the maximum depth of the river was 0.32-0.37m. The maximum flow speed was observed on July 31 and was 1.89m/s, the minimum rate was fixed on April 20 and was 0.13m/s.

The analysis of the runoff hydrograph for 2017 (Figure 2.3) showed that the main run-off for the vegetation period is in May-August, the beginning of the high water is in mid-May, the end is in the middle of September. During the vegetation period, the runoff of the Bash-Kaindy River consists of groundwater by 13%, of the melting of the seasonal snow cover by 57% and of the glaciers melting by 30%. According to these results, this river can be classified as snow and glacial type of feeding. In this regard, it should be noted that earlier studies [1] determine, in general, the snow-glacial type of feedingfor the At-Bashi River.
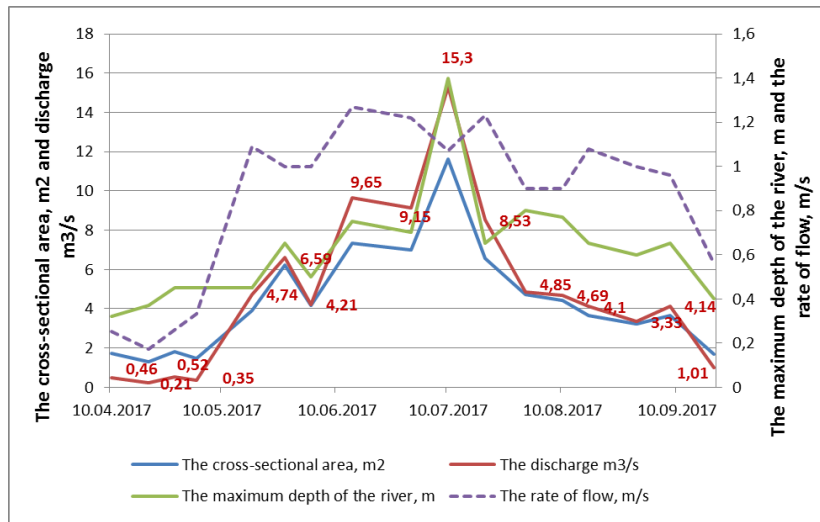
Fig.2.3. The main ten-day characteristics of the Bash-Kaindy River flow in 2017

Analysis of the combined hydrograph of the Bash-Kaindy River basin and air temperatures, according to the data from the At-Bashi MS and the AMS established in the basin of the Bash-Kaindy River in June (Fig. 2.4), shows depletion of the flow in August, while the air temperature rises and reaches its maximum values of 26.6^0C in the first decade and 23.3^0C in the second decade of August, which allows to conclude that in 2017 the most significant runoff was due to the melting of seasonal snow cover and to a lesser extent due to glaciers. Accumulation of precipitation in October-March and October-April 2017 according to the At-Bashi MS (currently it is the Kyrgyzhydromet's meteorological post) was 98% of the norm and 162% of the norm, respectively. In connection with this, the runoff on the rivers of the Naryn basin was increased. On this basis, it can be assumed that the runoff of the Bash-Kaindy River during the vegetation period of 2017 was also increased, comparing to the average runoff typical for this river.
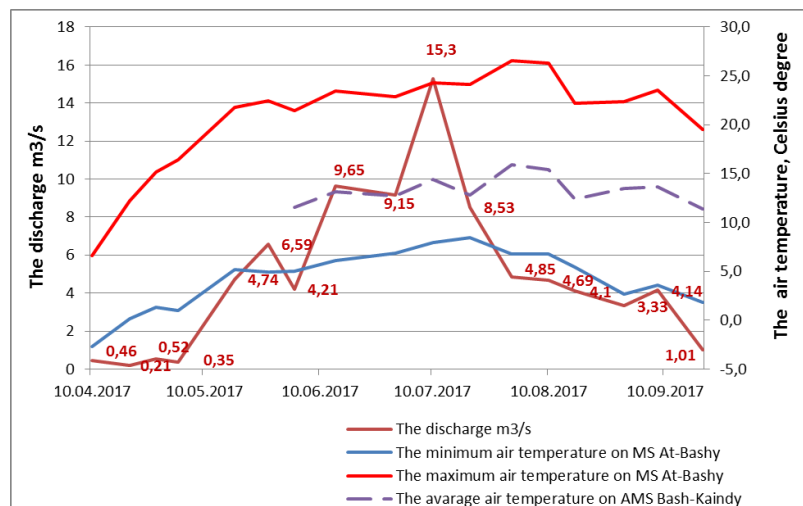
Fig.2.4. Alignment of the Bash-Kaindy River runoff hydrograph and the air temperature onthe At-Bashi MS and the Bash-Kaindy AMS.

Precipitation falling in the form of rain in June and July also contributed to the increase in river's runoff, but the decisive factor was the rise in air temperature and the melting of seasonal

snow cover (Fig. 2.5). According to the AMS data, established in Bash-Kaindy, the amount of precipitation in June-August was higher than according to the At-Bashi MS.
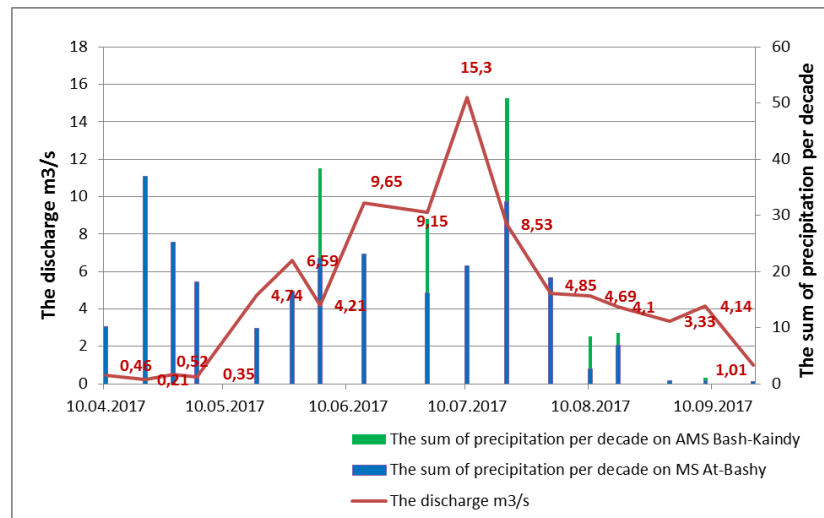
Fig.2.5. The combination of the Bash-Kaindy River runoff hydrograph and the amount of precipitationon the At-Bashi MS and the Bash-KaindyAMS.

3. Hydrochemical research

Hydrochemical studies are important for detection of water pollution by various chemicals that affect the quality of river water. Of particular interest is the assessment of water pollution by radioactive and rare-earth elements, as well as by heavy metals.

On October 19, 2016 samples of water were takenat three points, at various sites of the Bash-Kaindy River, (Figure 3.1). The laboratory analysis of these samples was carried out in the State Enterprise "Central Laboratory" under the State Agency for Geology and Mineral Resources under the Government of the Kyrgyz Republic.

Fig. 3.1. Places of water sampling from the Bash-Kaindy river. Points: No. 1 "Glacier" - from the stream of the No. 182 Glacier; No. 2 "Shakyr" - below the waterfall and No. 3 "Runoff" - the middle course of the Bash-Kaindy River, above the hydro-construction.

Tables 3.1, 3.2, 3.3 show the results of general chemical and spectral analysis of the river water samples.

Results of general chemical analysis

Element	ПДК, mg/l.	Unit	Content		
			№ 1 "Glacier"	№ 2 "Shakyr"	№ 3"Runoff"
Calcium	-	mg/dm^3	32	46	58
magnesium	-	mg/dm^3	4	6	11
potassium	-	mg/dm^3	<1,0	<1,0	1,0
Sodium	-	mg/dm^3	1,1	3,5	5,6
irontotal	0,3	mg/dm^3	0,105	0,1	0,1
ammonium	-	mg/dm^3	<0,1	<0,1	0,1
chlorides	350	mg/dm^3	4	6	9
sulfates	500	mg/dm^3	49,38	27,98	61,31
nitrates	45	mg/dm^3	2,5694	1,9492	2,3036
nitrites	3,3	mg/dm^3	0,01	0,01	0,01
bicarbonateion	-	mg/dm^3	57	142	146
carbonate-ion *	-	mg/dm^3	<1,5	<1,5	1,5
totalhardness	-	Mg/in dm^3 equivalent	1,97	2,8	3,8
Carbonatehardness		Mg/in dm^3 equivalent	0,93	2,33	2,4
Non-carbonatehardness		Mg/in dm^3 equivalent	1,04	0,47	1,4
silicicacid* H$_4$SiO$_4$	-	mg/dm^3	2,496	5,248	5,44
pH	-	-	7,70	8,20	7,80
Oxidability according to KMnO4 (according to consumed oxygen)	-	mg/dm^3	0,296	0,776	0,880
Dryresidue	-	mg/dm^3	137	184	248
Mineralization		mg/dm^3	165,5	255	321

Ion content in river water

Ions	№ 1 "Glacier"			№ 2 "Shakyr"			№ 3"Runoff"		
	mg/dm^3	Mg/in dm^3 equivalent	% mg/dm^3	mg/dm^3	Mg/in dm^3 equivalent	% mg/dm^3	mg/dm^3	Mg/in dm^3 equivalent	% mg/dm^3

Ca	32	1,6	78,8	46	2,3	78	58	2,9	71,8
Mg	4	0,37	18,2	6	0,5	16,9	11	0,9	22,3
Na	1,1	0,05	2,5	3,5	0,15	5,1	5,6	0,24	5,9
K	0	0,00	0	0	0,00	0	0	0,00	0
NH_4	<0,1			<0,1			<0,1		
Fe общее	0,105	0,01		<0,1			<0,1		
Cations	**37,205**	**2,03**		**55,5**	**2,95**		**74,6**	**4,04**	
Cl	4	0,1	4,8	6	0,16	5,2	9	0,24	6,1
SO_4	49,38	1,03	49	27,98	0,58	18,7	61,31	1,28	32,3
HCO_3	57	0,93	44,3	142	2,33	75,2	146	2,4	60,6
CO_3		<0,05			<0,05			<0,05	
NO_3	2,5694	0,04	1,9	1,9492	0,03	1	2,3036	0,04	1
NO_2	<0,01			<0,01			<0,01		
Anions	**112,95**	**2,1**		**177,93**	**3,1**		**218,61**	**3,96**	
Summ of cations & anions	**150,15**			**233,43**			**293,21**		

Table3.3

**ContentofheavymetalsinwatersamplesoftheBash-KaindyRiver,
accordingtotheresultsofspectralanalysis**

Chemical element	№ 1 |Glacier" mg/l	№ 2 "Shakyr" mg/l	№ 3 "Runoff" mg/l	Max.permis. concentration, mg/l
Mn	-	-	-	0,1
Ni	0,0008	0,0006	0,002	0,10
Co	-	-	-	0,10
Ti	-	-	-	0,1
V	-	-	-	0,10
Cr	-	-	0,004	0,5
Mo	-	-	-	0,25
W	-	-	-	0,05
Zr	-	-	-	-
Nb	-	-	-	-
Cu	0,0018	0,0025	0,0023	1
Pb	-			0,03
Ag	0,0002	0,0001	0,001	0,05
Sb	-	-	-	0,05
Bi	-	-	-	0,10

As	-	-	-	0,05
Zn	-	-	-	1
Cd	-	-	-	0,001
Sn	-	-	-	-
Ge	-	-	-	-
In	-	-	-	-
Ga	-	-	-	-
Yb	-	-	-	-
Y	-	-	-	-
La	-	-	-	-
Ce	-	-	-	0,01 [в
P	-	-	-	-
Be	-	-	-	0,0002
Sr	0,077	0,15	0,13	7,0
Ba	-	-	-	0,10
Li	-	-	-	0,0030
Th	-	-	-	-
U	-	-	-	1
Pt	-	-	-	-
Au	-	-	-	-
Sc	-	-	-	-

As the Tables 3.1 and 3.2 show, the water in the Bash-Kaindy River has low mineralization, low hardness, neutral and alkaline reaction by pH and hydrocarbonate-calcium ion composition. The insignificant increased sulfate ion content at the sampling point No. 1 may be due to the effect of sulphide mineralization in the rocks. In water samples, only five elements of heavy metals were found (Table 3.3).In this case, the chromium content (Cr) was found only in sample No. 3, in the middle course of the river. All the detected elements have a concentration value well below the maximum permissible value.Most elements of heavy metals could not be detected as they were beyond the sensitivity of spectral analysis. The detected heavy metals have a natural origin, and are not related to anthropogenic factors.Thus, the water of the Bash-Kaindy River, at least above the village of the same name, is quite suitable for domestic and drinking use.

Note that, taking into account the importance of water quality for the residents of the villagers and the need for an environmental assessment of the main sources of freshwater, such studies are to be continued on other parts of the Bash-Kaindy River and other rivers and streams of the aiyl's district.

4. Glaciological research.

In 2016-2017 the field research observations were made on glaciers in the basin of the Bash-Kaindy River, in particular, on the No. 182 [3] Glacier (Fig. 4.1). To plan field measurements and obtain additional information on glaciers, ultra-high resolution satellite images were used (Figure 4.2) Theablation stakes were set on the No.182 Glacier to measure the melting point of ice, and the first ablation parameters were obtained (Fig. 4.3). In addition, geodetic measurements of the height of the glacier'ssurface and mapping of its tongue's

boundary were performedusing GPS. (Fig.4.4). The estimation of the degree of moraine covering the glacier's tongue and its thickness was made.Itwas concluded that most of the glaciers of the northern slope of the At-Bashi ridge have a high degree of moraine cover of the end part of their tongues, with the continuous transition of modern moraine into ancient moraine deposits, which makes it difficult to diagnose the change in the area of the tongues.
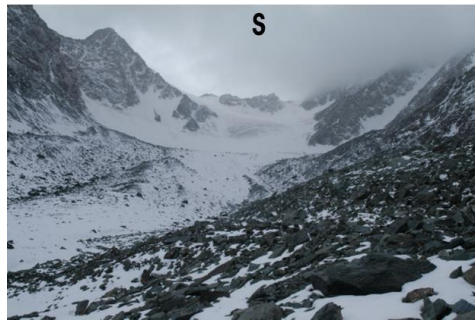
Fig. 4.1 The № 182 Glacier
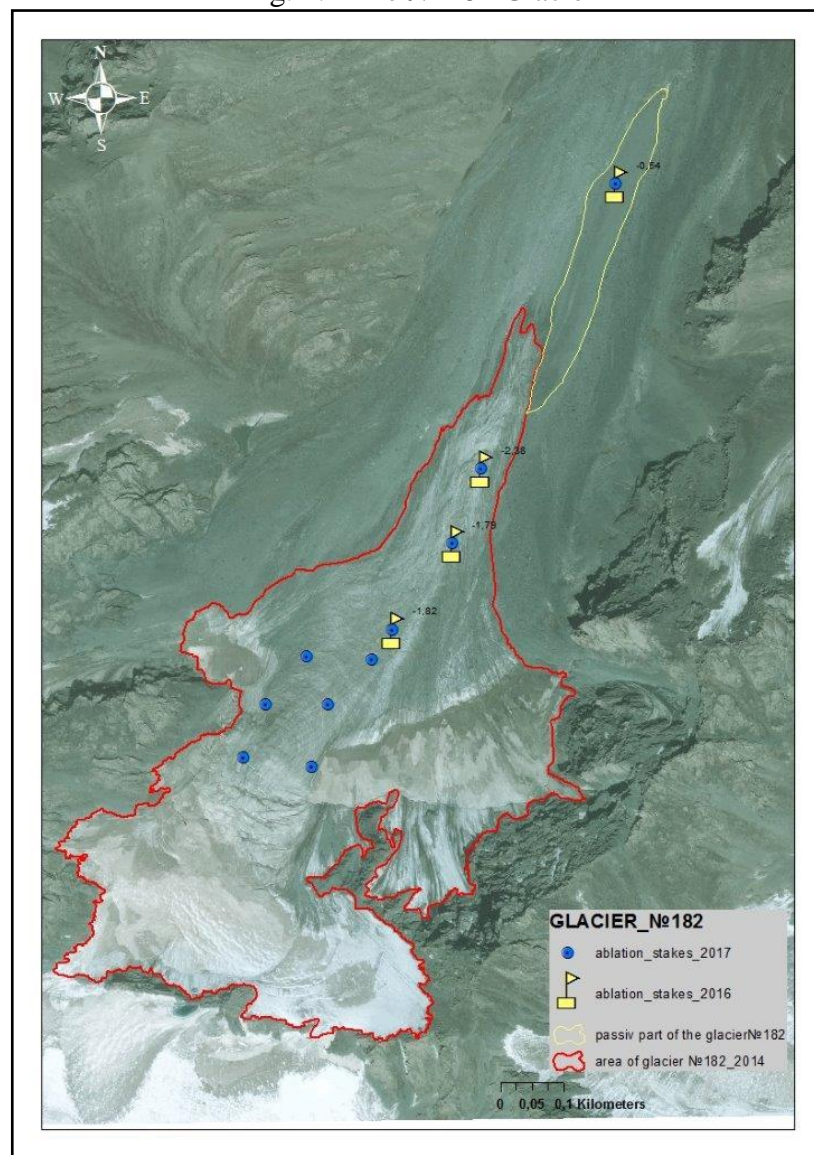
Fig.4.2 The No.182 Glacier on the "GeoEye-1" satellite image from August 1, 2014. The red line is the boundary of the glacier, the yellow line is the boundary of the passive part of the glacier separated from the active tongue of the glacier. The points are ablation rods installed in 2016 and 2017. Numbers are the ablation value in meters for the period 2016-2017.
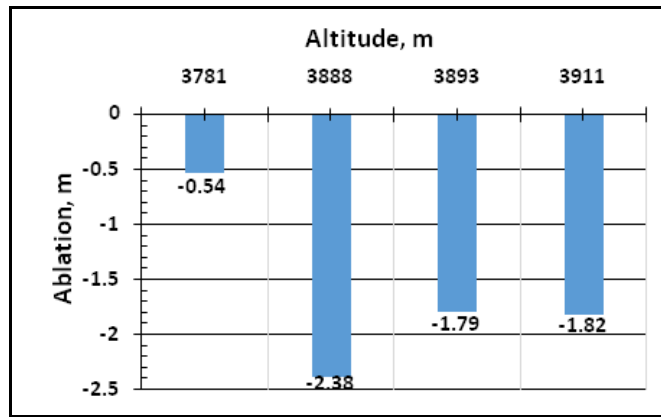
Fig. 4.3 The value of ablation of the No.182 Glacier for the period 2016-2017by different ablation stakes

Fig. 4.4 Geodetic measurements on the No.182 Glacier

1.2 The results of the analysis of published data, decoding of space images in 2016-17.

1.Meteorological research

In the area of the study, the main source of meteorological information is the At-Bashi meteorological station of Kyrgyzhydromet, located at an altitude of 2,025 meters above sea level, operating since 1927 and currently having the status of a meteorological station (MS). At this station, a complex of observations was carried out and is still carried out, including the measurement of the main parameters: the temperature of the surface air layer and the amount of atmospheric precipitation. Figure 1.1 shows the change in the average annual air temperature for the At-Bashi MS over 58 years. As follows from this graph, the air temperature over the entire observation period varied in the range from 0.3 to 4 ° C and, in the presence of irregular periodic oscillations, had a tendency to increase by a linear trend by approximately 1.5 ° C, that is, the gradient of increase in average temperatures is 0.026°C /year. This trend can be predicted for the next decade.
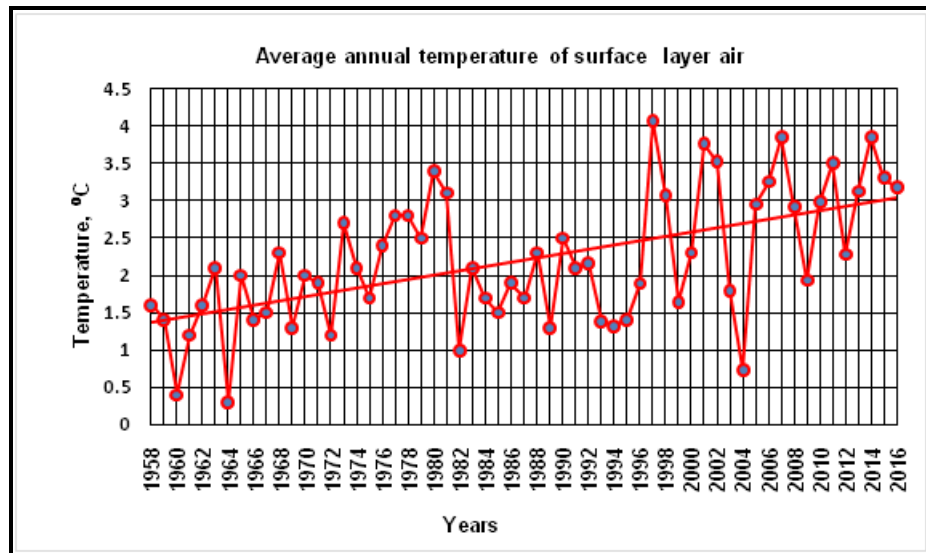
Fig.1.1 Average annual surface air temperature at the At-Bashi MS

At the same time, attention should be paid to the presence within the observed period from 1982 to 1996, with a relative temperature decrease of 0.5-0.7°C for 14 years. This period was preceded by a high-amplitude decrease in temperature, and after the completion of the low-temperature period, a high-amplitude change in the mean annual temperatures till2007 with the subsequent reduction of amplitudes to the values that were at the beginning of the entire observation period. This corresponds to the irregular periodic cyclic change in the average annual temperatures with a period of about 30 years and the possibility of the next repetition of the relative decrease in temperatures around 2022.

Atmospheric precipitation at the At-Bashi MS as it's seen in Figure 1.2, for a period of 75 years from 1940 to 2015, have a weak linear trend to increase. The minimum value of the sum of annual precipitation (SAP) for the entire observation period is 117 mm, the maximum value is 535 mm; most of the SAP is in the range of 200-400 mm. The maximum amplitude of changes in the SAP at the beginning of the observations is 166-200 mm, and in the last years of the observation period is about 200-250 mm. In the aspect of the forecast, it seems a reasonable guess that the tendency of a slight increase in precipitation and the nature of change in their amplitudes in the next decade will remain.
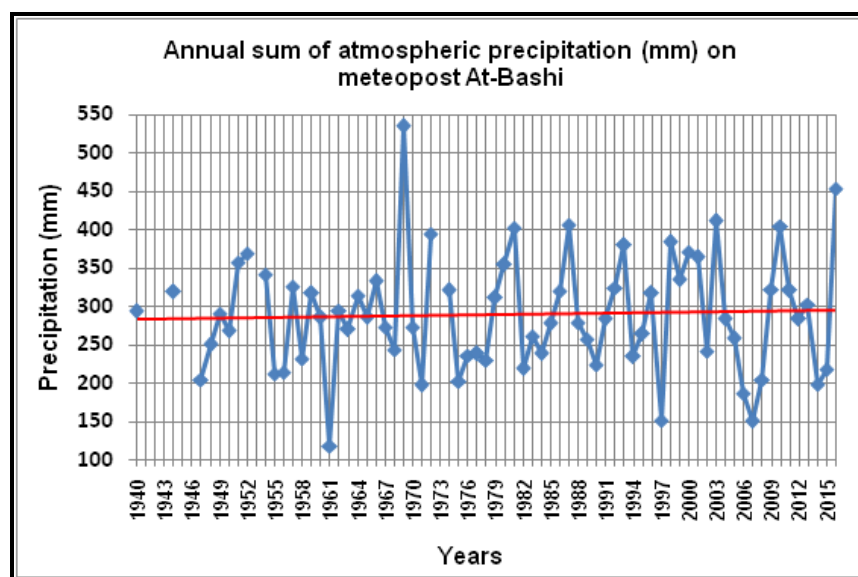
Fig. 1.2 Annual sums of precipitation by the At-Bashi meteorological station (previously weather station).

2. Hydrological research

2.1 Nature of the At-Bashi River runoff change according to instrumental observations from 1937 to 1995.

An analysis of the At-Bashi River runoff change was made based on the results of measuring water discharge in the river at the Acha-Comandy River Estuary gauging station in the interim from 1937 to 1995. For this station, the average absolute height of the catchment area is 3500 m, the catchment area is 1500 km^2. Figure 2.1.1 shows the water discharge in the river from 1942 to 1994.
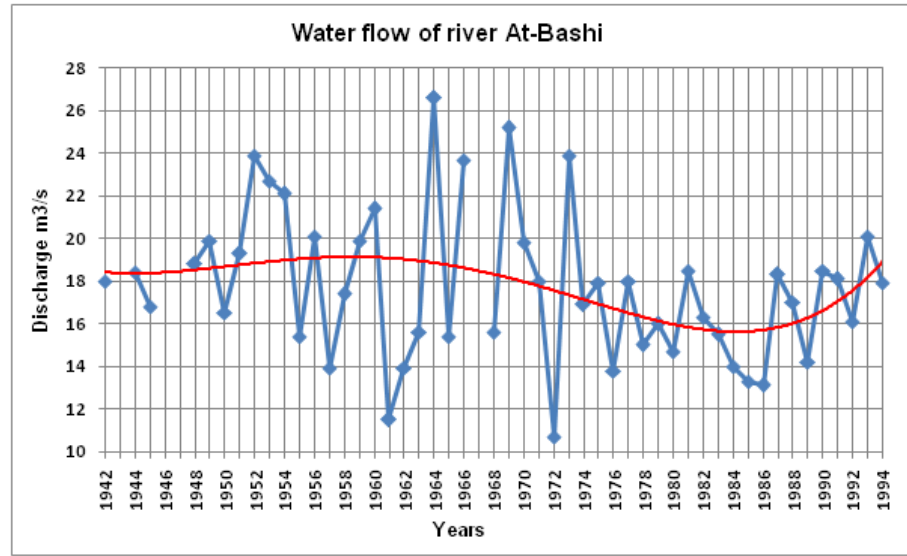
Fig. 2.1.1 Average annual water discharge in the At-Bashi River for 52 years.

As can be seen in Figure 2.1.1 over the considered period, a significant irregularity in the water discharge of the At-Bashi River was observed, which manifested itself in a significant amplitude of fluctuations in the average annual runoff in the period from 1951 to 1974. Before the beginning of this period and later, the amplitude was several times smaller. This indicates a significant change in the conditions for the formation of the hydrological system with their subsequent return to their original state. Obviously, such a situation is possible in the foreseen future.

Distribution of various water discharge rates in the At-Bashi River over the 47-year period from 1948 to 1995 is shown the graph in Figure 2.1.2. The probability of discharge of 10 m^3 /sec = 46%, 80 m^3 / sec = 0.35% (total 569 cases).
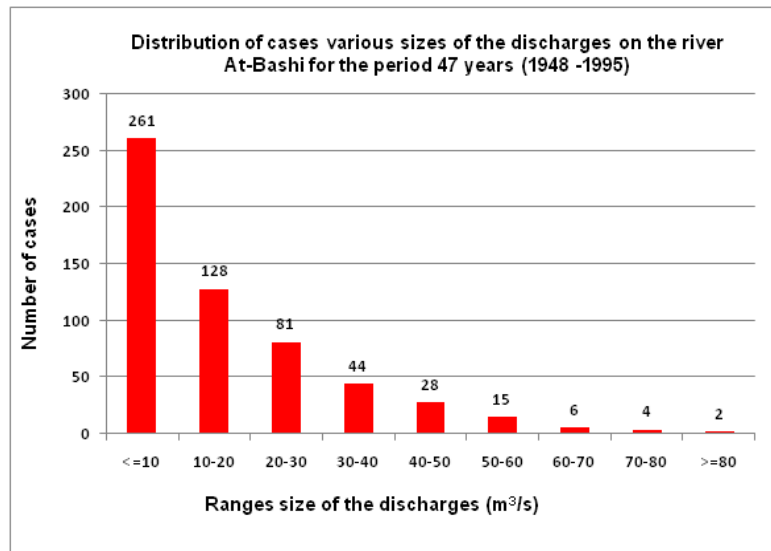
Fig. 2.1.2. Distribution of various water discharge rates in the At-Bashi River over a period of 47 years from 1948 to 1995.

In terms of possible negative impact of global and local warming on development of dangerous hydrological processes, an analysis of the nature of change in the maximum multi-years river runoff in June and July for the period from 1938 to 1995 was made The results of the analysis shown in Figure 2.1.3 indicate that the trend of extreme events associated with the maximum summer discharge of the At-Bashi River has, according to available data, an irregular periodicity of several dozens of years, with highs and lows alternating in 25 - 30 years. An important result of this analysis is that during the considered period, in the At-Bashi River basin, there is no clear trend of an increase in extreme events caused by the maximum summer discharge due to climatic changes.
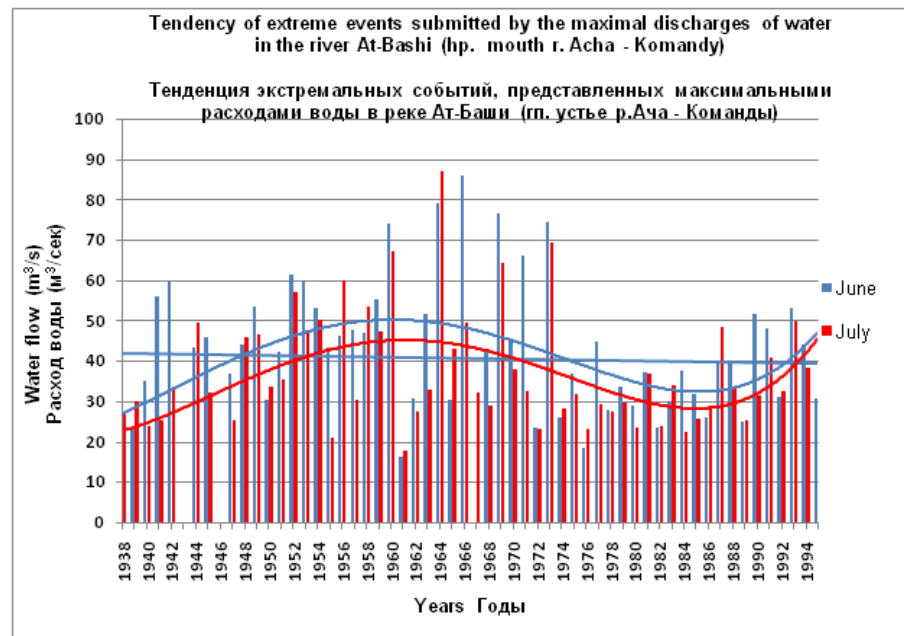
Fig. 2.1.3 Long-term change in the maximum summer discharge of the At-Bashi River

2.2 Analysis of channel processes in the valley of the At-Bashi River near the village of Bash-Kaindy

The analysis of channel processes in the valley of the At-Bashi River was carried out in order to determine the risk of possible erosion and collapse of the southern steep bank of the At-Bashi

14

River, which is a northern boarder of the territory of Bash-Kaindy village along 1500m. The nature of channel processes in the valley of the At-Bashi River is determined by the results of interpretation of various space images obtained at different times and by topographic maps.

The analysis of the topographic map (Fig.2.2.1) of scale 1: 100000, published in 1985 and reflecting the state of the terrain for 1963, showed that in the valley of the At-Bashi River, for the considered period, the riverbed of the At-Bashi River near Bash-Kaindy village did not have one main channel, but was represented by a ramified branch system with a total width of 100 - 330 m and located at a distance of 80-90m to 300m from the cliff of the southern bank. Such channel configuration indicates that in the considered part of the river, the accumulation of river's sediments predominated, that is, the accumulation processes prevailed over the erosion processes. Only one small southern channel approached to the southern bank in the eastern part of the site, which has the main feed from the groundwater, emerging to the surface in the form of "Kara-Suu" creeks on the terraces above the floodplain east of the village. Thus, there was no risk of the northern bank caving and collapse.
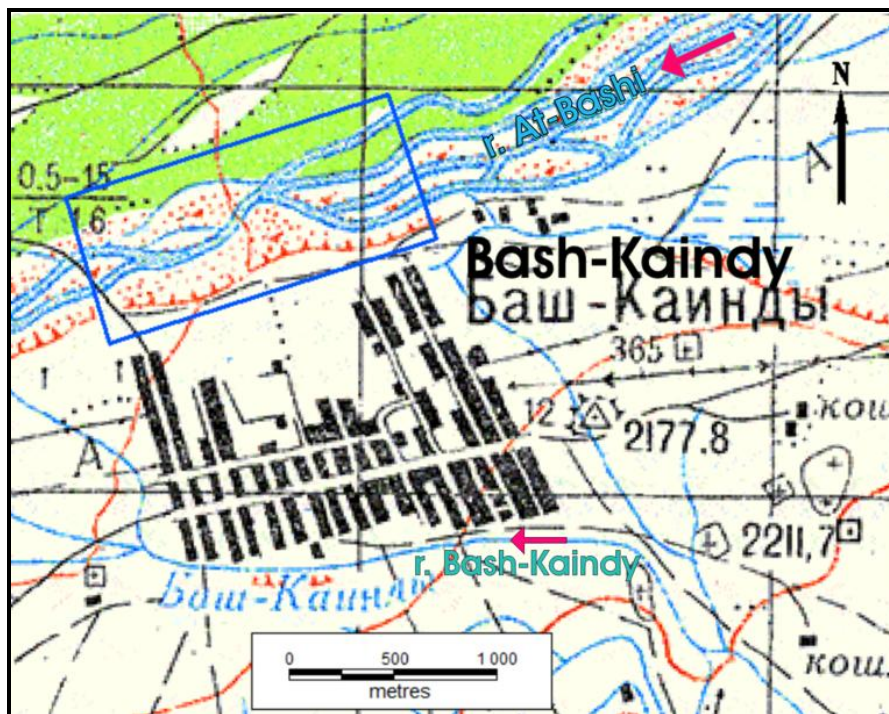
Fig.2.2.1 The blue rectangle frames a section of interest in the area of of Bash-Kaindy village. Red arrow indicates direction of the river's flow.

The situation considered above on the topographic map does not have a detailed temporal monthly detailed reference. In contrast, the space images allow us to reflect the processes that are of interest to us and have the greater temporal detail. For the analysis of channel processes, the months with the maximum water discharge in the At-Bashi River are the most interesting. According to Kyrgyzhydromet, the Acha-Comandy River Estuary hydro gauge station, which operated from 1937 to 1995, shows the largest water discharge in the At-Bashi River in June and July, as shown in Figure 2.2.2.
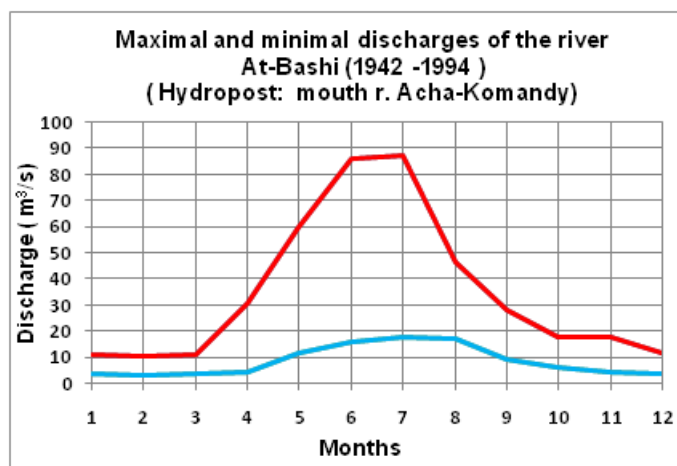
Fig.2.2.2 Average monthly water discharge in the At-Bashi River from 1942 to 1994.

According to this, for further analysis, the "Pleiades" satellite images from July 27, 2013 and May 21, 2016, received from the "Google Eart" service, reflecting the configuration of the channels in the months of maximum water discharge in the river were used. Note that the image of 2016 is considered first, since it is better to discern the channel network.

The configuration of the At-Bashi River riverbed in May 2016, in the valley near the village of Bash-Kaindy, is shown in Figure 2.2.3. Here on the "Pleiades" satellite image from May 21, 2016, the situation is close to that which was earlier in 1963, based on the result of the topographic map analysis. The image shows that in the last decade of May 2016, the main channel is represented in the same way as in the past: by a network of channels located at a distance of 270-330 m from the northern bank. Near the northern bank is the secondary channel along which the runoff flows, mainly, from the groundwater from the creeks of "Kara-Suu" type. This channel approaches the southern bank most closely, at a distance of 20 – 45m, in a section about 160 m long and along this section forms a channel approaching the bank cliff directly. The erosional activity of this riverbed and the activity of the channel are insignificant due to feeding from the groundwater, for this reason they do not pose a real threat in the aspect of the northern bank caving, as the main course of the river, as already noted, is located much farther north. The detailed fragment of this section of the river valley is shown in Figure 2.2.4.

In 2013, the pattern of distribution of riverbed channels of the At-Bashi River in the period of high water or maximum water discharge was obtained from the Pleiades satellite image dated July 27, 2013 (Fig. 2.2.5). The image shows that the configuration of the riverbed channels remains practically constant, but at high discharge rates, part of the main runoff goes not only along the main riverbed, but also along the secondary channel, as shown in Fig. 2.2.6.

Thus, the comparison of the different positions of the riverbed during the 53-year period indicates that the configuration of the riverbed observed at this site is stable and will remain for decades. It does not pose the risk of the northern shore caving and its collapse, even in the segment of the minimum distance from the riverbed to the bank.

In this case, preventive measures can strengthen the protection of the northern bank from possible negative impacts of the river in the future.

The main measures include:

1. The construction of dams regulating the direction of runoff of the secondary channel directly near the bank, in particular, the dam of about 100 m long (Fig.2.2.4).

16

2. Forest reclamation measures are recommended to be performed by planting shrub vegetation of high density (in checkerboard pattern) in the floodplain, immediately below the cliff, at a length of about 340 m along the northern bank, along the mentioned channel (Fig. 2.2.4) and increase the density of existing plantations on this site over 620 m. This will in the future protect the northern bank from caving and collapsing, as shrub vegetation, in case of flooding by river flows, will reduce the rate of their current and accumulate river's sediments.

3. The extreme upper part of the steep northern bank should be protected from uncontrolled surface runoff of irrigation and other waters to prevent the formation of the gullies. To do this, it is recommended to build a catchment ditch along the bank near the village with an over flow chute. In addition, the uppermost part of the steep northern bank can be fixed with perennial grasses, forming a vegetable layer and shrubbery.
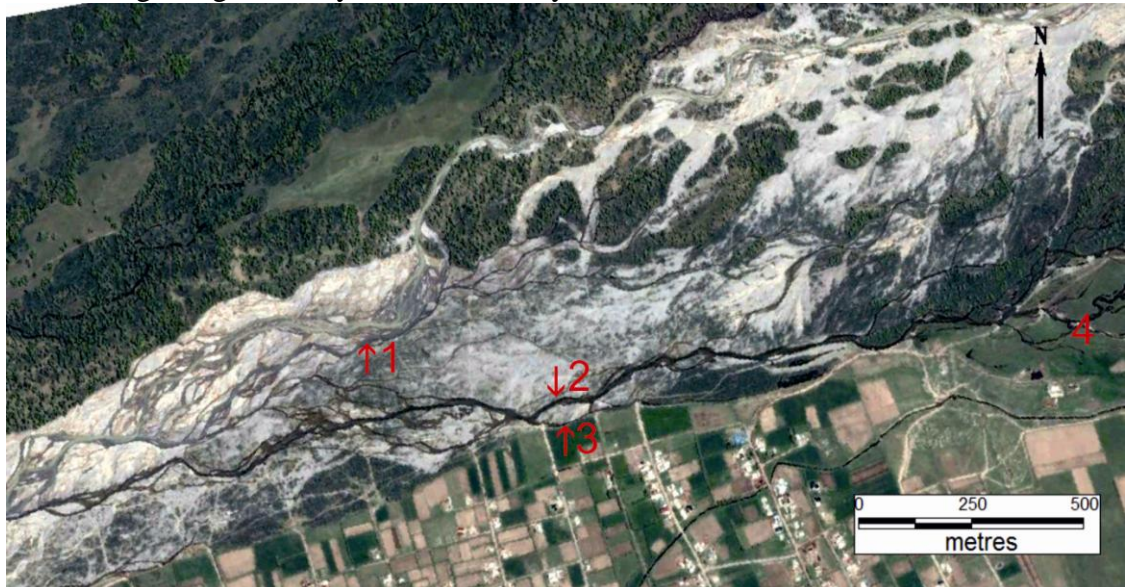
Fig.2.2.3 The "Pleiades" satellite image from May 21, 2016. 1-main riverbed of the At-Bashi River, 2 - secondary channel, 3-channel, approaching directly to the bank, 4- sources of "Kara-Suu" creeks feeding the secondary channel.

Fig.2.2.4. A fragment of the space image of 2016, showing the channel passing under the riverbank slope. The red line is a project dam about 100 m long. The green dotted line is a bush planting area.
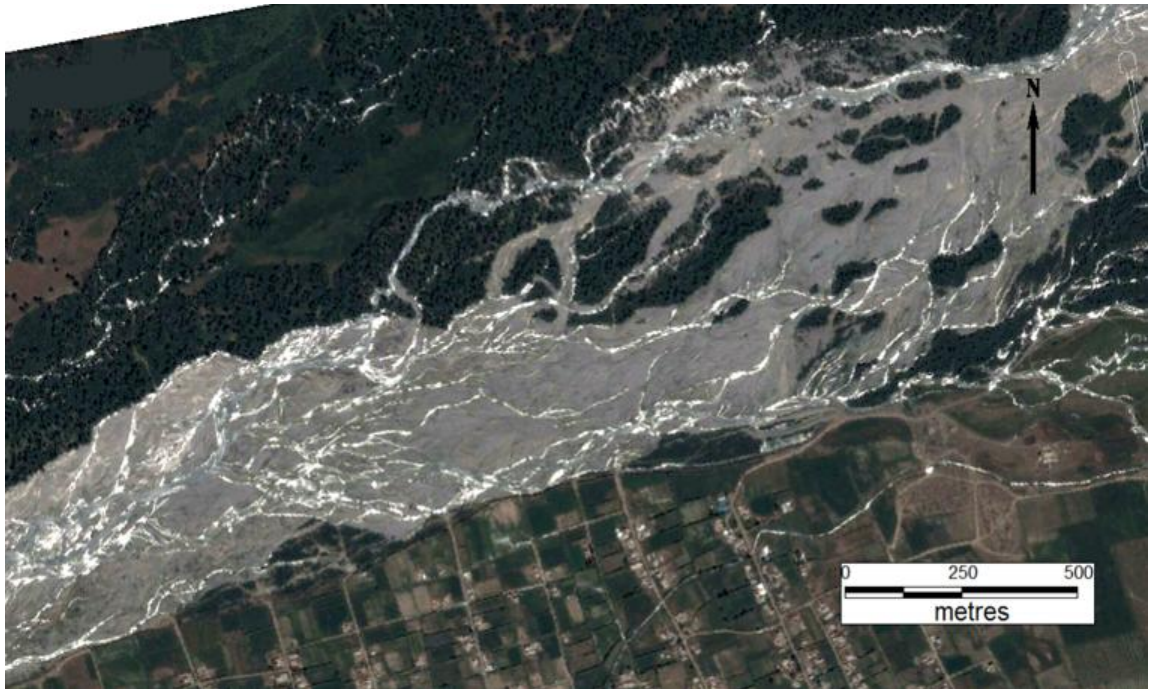
Fig.2.2.5 Space image of the "Pleiades" satellite from 07/27/2013

Fig. 2.2.6. A fragment of a satellite image from 2013, showing the channel passing under the riverbank slope

3. Glaciological research.

Studies of changes in the glaciers within the At-Bashi Basin were carried out by interpreting the "Landsat 8" satellite images, performed in 2013-2015 and the results were compared with the information on glaciers contained in the Glaciers Catalog of the USSR, Volume 14, Issue 1, Part 6, 1974 [3]. "Landsat 8" satellite images were obtained from the American Geological Service USGS - https: //earthexplorer.usgs. gov /.In addition, published topographic maps were used for

analysis, mainly on a scale of 1: 100,000, as well as a digital relief model (DRM), with a resolution of 30 meters, built from the ASTER radiometer, located on the TERRA satellite, obtained from the website of the US National Aerospace Agency (NASA) - http://earthdata.nasa.gov/.

To interpret the space images, a combination of 4,5,6 channels was used: red visible and near, medium infrared. The resolution of the obtained images was increased by using the 8th panchromatic channel up to 15 m/pixel. These transformations were performed in the ENVI 4.6.1 software package. Mapping and calculation of morphometric characteristics were carried out in GIS MapInfo Professional 7.8. The results of the analysis of changes in glaciers in the At-Bashi and other ridges of the At-Bashi basin for 41 years from 1974 to 2015 are shown in Table 3.1.

Table 3.1

	Total number of galciers in the Atbashi River basin		Size of glaciers > 0.1 km^2		Size of glaciers < 0.1 km^2	
	Number	Area km^2	Number	Area km^2	Number	Area km^2
By Catalogue	284	113,7	253	112,2	31	1,5
By Landsat 8	303	84,1	174	78,0	129	6,1
	+6,3%	-26%	-31,2%	-30,5%	+75,9%	+75,4%

As follows from the Table 3.1, the total area of the glaciers in the ridges of the At-Bashi basin decreased by 41% in 41 years, while the number of the glaciers increased by 6.3%. Thus, the reduction rate is 0.6%/year. The increase in the number of glaciers is associated with the decay of the large glaciers into smaller ones, as evidenced by a decrease in the number and area of the glaciers larger than 0.1 km^2 and an increase in the number and area of the glaciers smaller than 0.1 km^2.The location of the glaciers in the Bash-Kaindy River basin, on the northern slope of the At-Bashi Ridge, is shown in Figure 3.1. The numbers of glaciers in this scheme correspond to the numbers of the Catalog of Glaciers of the USSR [3]. The parameters of change in these glaciers are included in the mentioned above results of change in glaciers in general in the basin of the At-Bashi river. Specifically, in the basin of the Bash-Kaindy River, as can be seen from the Table 3.2, the area of glaciers in the interim from 1974 to 2015, decreased by 1.1km^2:from 3 km^2 to 1.9 km^2, or by 36.7%, with a decrease rate of 0.9 %/year or 0.027 km^2/year, for the considered period of time. The number of glaciers larger than 0.1 km^2 decreased from 10 to 8, that is, by 20%.At the same time, while decoding, one glacier of 0.1 km^2 (No. 179-1) and 10 glaciers smaller than 0, 1 km^2, with a total area of 0.4 km^2 were discovered. They are not available in the Catalog of Glaciers of the USSR, that is, previously they were not recorded. They are not shown in the Table 3.2 because of their small size, but taking into account their area, the total glaciers area in the basin of the Bash-Kaindy River will be 2.3 km^2, and the difference in the areas will be 0.7 km^2.

Fig.3.1 Scheme of the glaciers location in the Bash-Kaindy River basin

Table 3.2

№ of glacier by the Catalogue	Area by Catalogue (km^2)	Are by sattellite (km^2)	Difference in areas (km^2)
175	0,4	0,5	+0,1(+20%)
176	0,1	0,0	-0,1 (-100%)
177	0,4	0,2	-0,2 (-50%)
178	0,3	0,1	-0,2 (-67%)
179	0,7	0,3	-0,4 (-57%)
179-1	0,0	0,1	+0,1 (+100%)
180	0,3	0,3	0,0 (0,0%)
181	0,2	0,1	-0,1 (-50%)
182	0,4	0,3	-0,1(-25%)
183	0,1	0,0	-0,1(-100%)
184	0,1	0,0	-0,1(-100%)
Total area of the Bash Kaindy River basin	3,0	1,9	-1,1(-36,7%)

Besides, three glaciers No. 176, 183,184 have not been detected possibly due to complete thawing and on the No. 178 glacier an area increase of 20% has been determined; the area of the No. 180 glacier has not changed. On the No. 182 glacier, which was selected for the field observations, the area reduced by 25%.

Thus, the results of the interpretation of the "Landsat 8" satellite images with a minimum error of 15m allowed to determine the boundaries of glaciers as of 2013-15 and their corresponding areas. At the same time, to determine the change in the glaciers area, which tongues are covered with moraine, the boundaries of the glaciers were drawn along the border of the open ice. In the Bash-Kaindy basin, a different character of changes in glaciers with respect to their parameters has been revealed by the Catalog of Glaciers of the USSR, depending on their size, exposure, and other factors. In general, the glacier area shrinks by 36.7%, but the reduction range is quite large from 25% to 67% for relatively large glaciers and to complete extinction (100%) for relatively small glaciers. At the same time, individual glaciers did not change their size, or even increased by 20%.

In addition to comparing the glacier parameters by the Catalog of Glaciers of the USSR and by the results of interpretation of the "Landsat 8" images, a comparison of change in the glacier area in the basin of the Bash-Kaindy River for 23 years from 1994 to 2017 was made by the "Landsat 4"TM and "Landsat 8" images.

As a result, it was found out that for the indicated period of time, the area of glaciers decreased by 12% or 0.5%/year, which is less than the speed defined above comparing to the CGU (catalog of glaciers of the USSR) - 0.9%/year, but close to the speed of area decreasing in general for the At-Bashi basin - 0.6%/year.

A determination of change in the glaciers' area was made depending on the absolute glacier's height (Fig. 3.2).
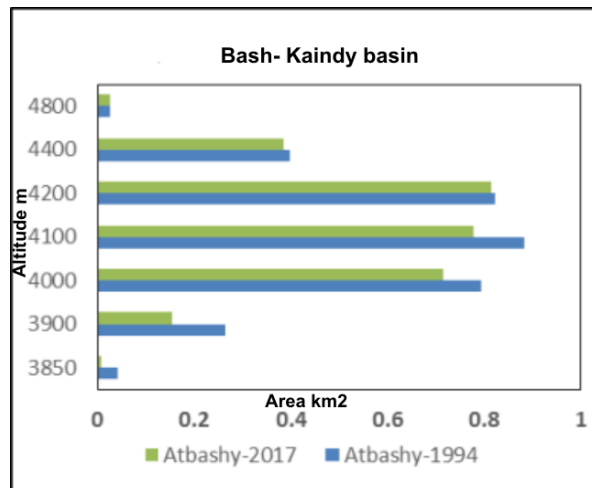
Fig.3.2 Change in the area of glaciers, depending on the altitude

At present, in the process of interpreting space images, a digital map of the boundaries of glaciers in the At-Bashi River basin was created as of 2013-15, which can be the basis for the subsequent study of changes in glaciers in this area.

2. *Pilot site 2.* Tajikistan, Gorno-Badakhshan oblast (GBAO), Rushan district, villages of Siponj-Khadorzhv and Darjomch (joomat Siponj).

2.1 Results of field works- 2017.

1.Meteorological research

During the field works in Tajikistan, in the West Pamir, near the village of Hijez (Fig.1.1, 1.2,1.3), by agreement with Tajikhydromet, an automatic meteorological station (AMS) was installed on August 7, 2017, transmitting the meteorological parameters to the CAIAG through the cellular network . The technical characteristics of the AMS are given in the Appendix 1.

Fig.1.1. Geographical location of the AMS in the village of Hijez.
Coordinates: 71.83.07 el; 38.0007nl, elevation above sea level - 2127 m. It is located at a distance of 7.5 km south - west from a temporary gauging station on the Siponj River.

Fig.1.2. Location of the AMS: south-western part of the Hijez village, area of inflow of the left tributary of the Bartang River - the Hejez River.

Fig.1.3. AMS view

In the period under review, the main meteorological parameters were obtained at the AMS: air temperature, relative humidity and atmospheric precipitation. In the period from October 17 to November 21, 2017 (34 days), the AMS did not work because of the lack of electricity. After November 22, the station was transferred into winter mode. In addition to the AMS data, in 2017, with the help of a local observer in the village of Sipongzh (Bartang), measurements of atmospheric precipitation were taken using a measuring vessel. They were also used to analyze the hydro meteorological conditions of the explored area, in particular for analyzing changes in the hydrological situation, and are presented in the hydrological section of this report.

2.Hydrological research

The Darzhomdara River is one of the numerous left tributaries of the Bartang River, originating from the No. 783 Glacier [4]. The water of this river is used both for drinking and for domestic purposes, for irrigation of orchards and gardens of the Darzhomch village residents. Unused water come directly to the Bartang River.

Measurement of the water discharge of the Darzhomdara River was taken only once for test purposes, by the float method on 08.08, 2017, in sunny and warm weather conditions, i.e. in the conditions of intensive melting of the glacier. The general hydrological conditions at the discharge measurement area are shown in Figures 2.1, 2.2, 2.3, 2.4, 2.5, 2.6, 2.7. Hydrometric measurements and water discharge calculation in the river were carried out by the method described in [2].

Fig.2.1. Water intake in Darzhomch village.

Fig.2.2. The Darzhomdara River (above the Darzhomch village)

Fig. 2.3. The place where the water discharge was measured on the Darzhomdara River, is one of the most suitable for hydrometric operations.

Fig. 2.4. Measurement of the width of the Darzhomdara River.

Fig.2.5. Determination of the depth of the Darzhomdara River.

Fig.2.6. Water intake into the irrigation canal from the Darzhomdara River.

Fig. 2.7 Scheme of the location of the explored objects.

Result of the water discharge calculation in the Darzhomdara River
.

Date: 08/08/2017

Length of the working hydrologicsection:10 m.

Width of the river: 2.0 m.

Depth of the river: 0.38 m, along the whole width of the river.

Flowing area: $\omega = 0,76$ m^2.

Maxspeed: $V_{max} = 9.16$ m/s.

Average speed:$V_{aver}= 1.19$ m/s.

Calculation of the actual water discharge in the river was carried out by the method recommended in [1].

Fictitious water discharge: $Q_{fic.} = V_{max} * \Omega = 6.96$ m^3/s

Transition code: $K = V_{aver}/V_{max} = 0.13$

Actual water discharge $Q = K * Q_{fic.} = 0.9048$m^3/s.

Note: above the hydrological site, water is collected for irrigation of the nearest field under the crop, with water discharge rates up to about 0.05-0.1 m^3/s (Figs. 2.6, 2.7).

The Khodorzhiodara River is one of the numerous right tributaries of the Bartang River, originating from the No. 19-22 through [4] glaciers; the view of this river in the lower reaches is shown in Figure 2.8.

Fig. 2.8. The Khodorzhiodara River

Partly the water of the Khodorzhiodara River is used by a small hydroelectric power station that provides electricity to several nearby settlements along the Bartang River valley. The diameter of the drainage pipe for water supply to the power station is 400 mm. Part of the water is taken for irrigation of the gardens and orchards of the Siponj village residents. Most of the water comes directly to the Bartang River (Figure 2.9, 2.10, 2.11). It should be noted that in winter, the water discharge in the river is often insufficient to operate the power station at a full capacity.

Рис. 2.9. Water intake on the Khodorzhiodara River for small power station
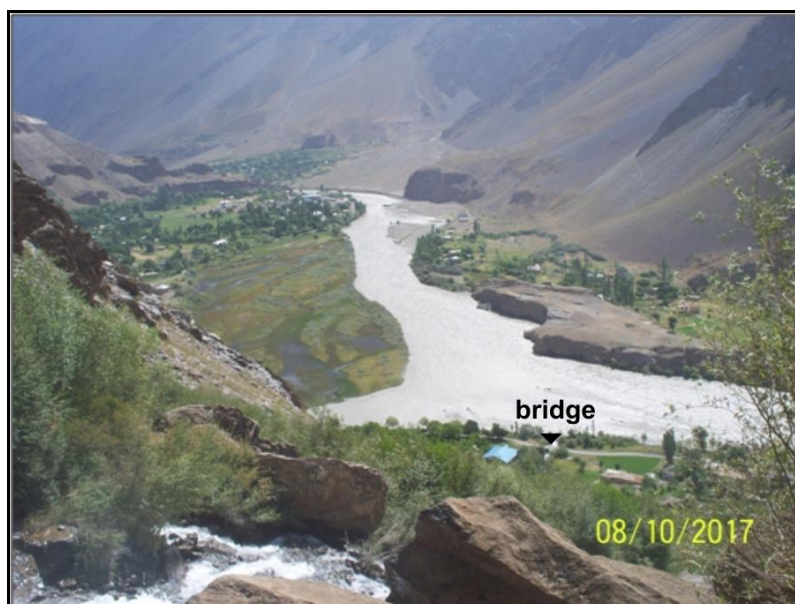
Рис. 2.10. Rivers Khodorzhiodara (in front) and Bartang (in the background).
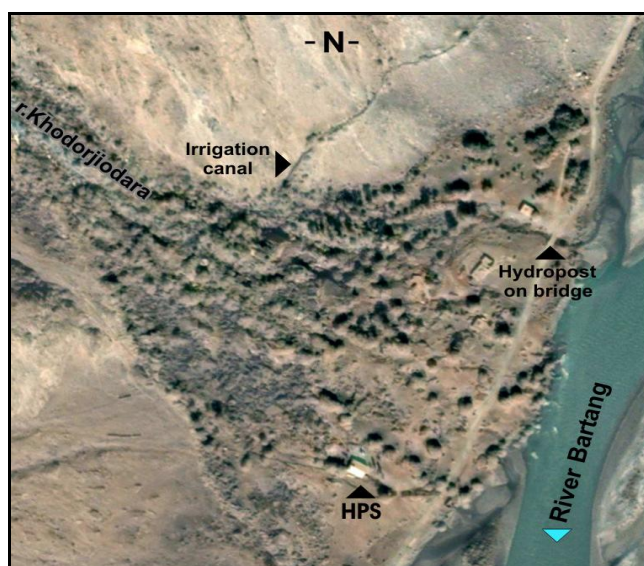
Fig.2.11. Scheme of the explored objects location.

Measurement of water discharge in the Khodorzhiodara River was carried out on a temporary stream gauge, organized on a transport bridge (Figure 2.11, 2.12, 2.13), located before the inflow of the Khodorzhiodara River in the Bartang River. This is the most convenient place for such task.

Fig. 2.12. Stake for measuring the water level in the Khodorzhiodara River on the stream gauge, on the bridge.

Fig.2.13 Bridge over the Khodorzhiodara River

Like on the Darzhomdara River, measuring the discharge rate of the Khodorzhiodara River was carried out by the float method, every 5 days, in the interim from August 10 to November 20, 2017. The parameters of the stream gauge on the Khodorzhiodara River under the bridge are as follows: length of the working stream gauge is 10 m. Width of the river or the stream gauge is 3.0 m. The maximum depth of the river is 0.55 m. During the observation period, the average water discharge was 1.59 m^3/s. Pentad discharge rate of the Khodorzhiodara River is shown in Figure 2.14.
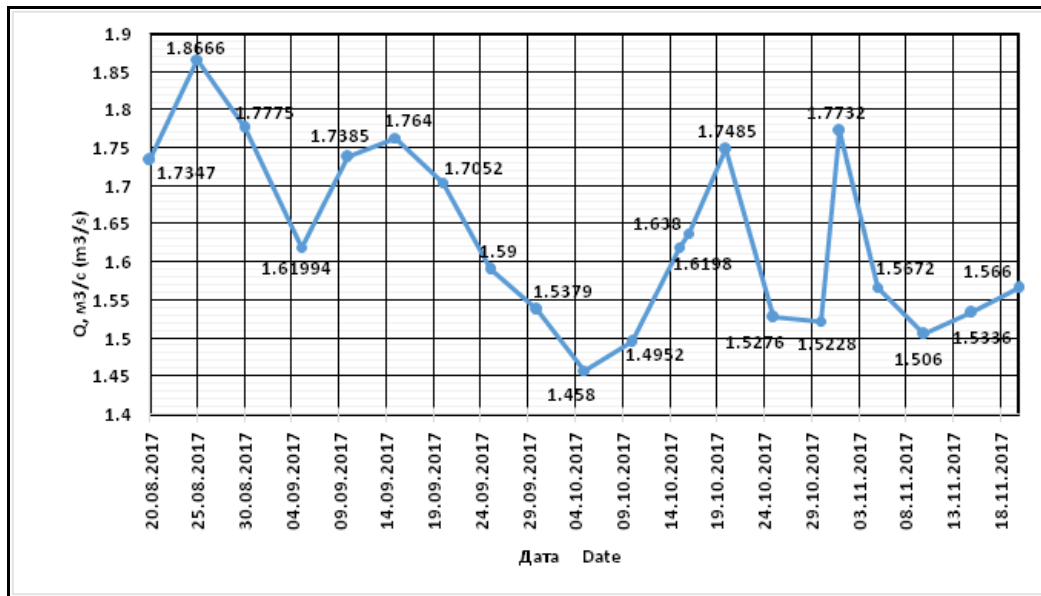
Fig. 2.14. The course of water discharge in the Khodorzhiodara River.

As can be seen from Figure 2.14, the maximum water discharge (1.9 m^3/s) was observed in the end of August, and then it began to decline. The next relatively high water discharge was recorded in mid-September, possibly due to a relatively short-term rise in air temperature (Fig. 2.15), then it gradually decreased in accordance with weather conditions without precipitation and with a drop in air temperature. Subsequent relatively high water discharge in the river may be due to precipitation. This is confirmed both by the "Hijez" AMS data and the measurement results of the local observer, according to which, the relative air humidity in the pilot region began to rise sharply from mid-September (Fig. 2.16); and in the first half of October the first precipitations began to fall (13,8 mm), which influenced the autumn increase in water discharge in the Khodorzhiodara River.

.
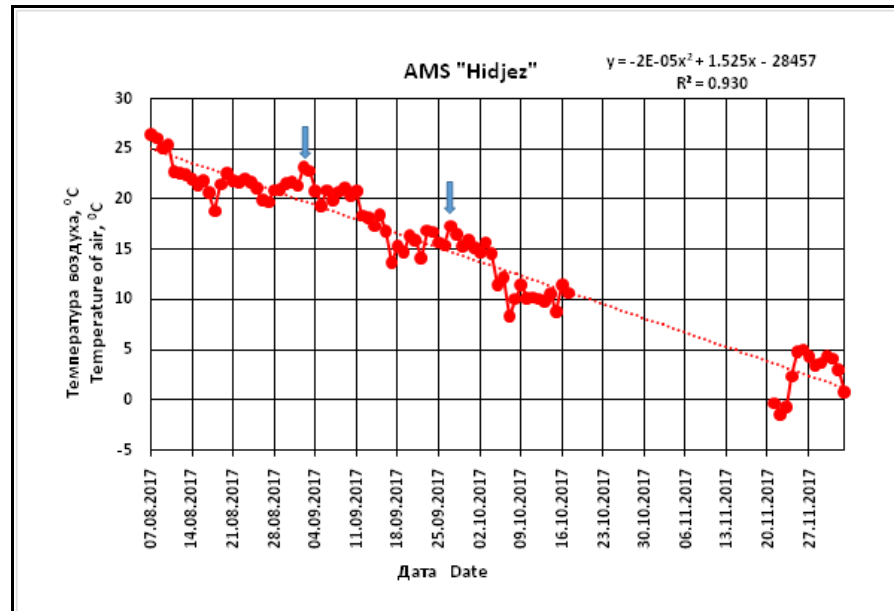
Fig. 2.15 Temperature of the surface air according to the "Hijez" AMS data. The blue arrows show the temperature maximum relative increase.
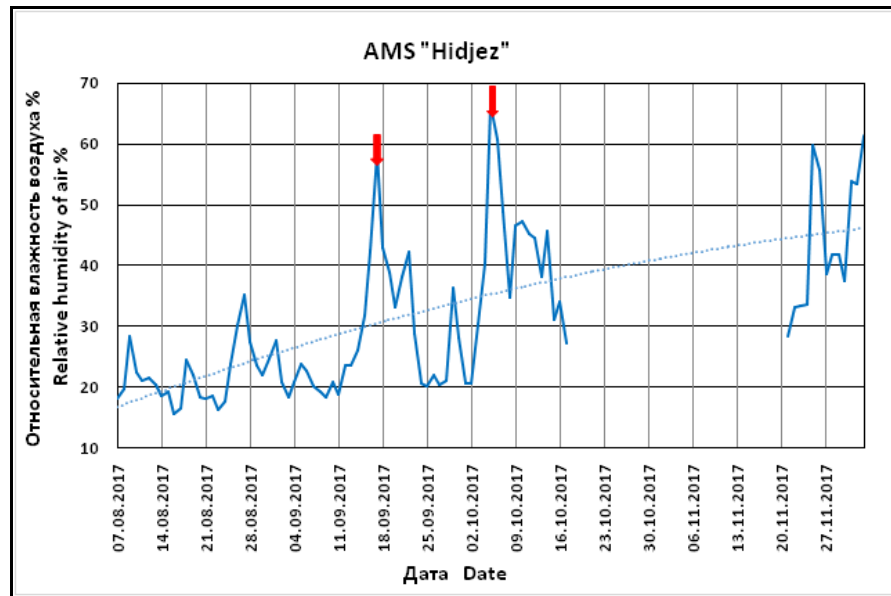
Fig.2.16 Relative air humidity according to the "Hijez" AMS data. Red arrows show the humidity maximum increase.
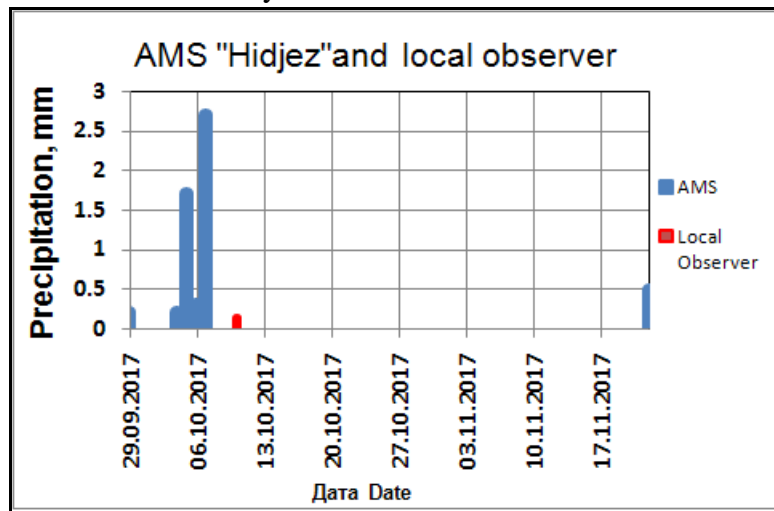
Fig. 2.17 Atmospheric precipitation according to the "Hijez" AMS data and the local observer in the Siponj village (Bartang).

In addition, the relative increase and fluctuations in the water discharge of the Khodorzhiodara River on the stream gauge on the bridge, starting from the first decade of October, may be due to the suspension of water intake or partial water intake above the stream gauuage, during repairs and emergency situations at the power station, before the beginning of the winter season. For example, on October 16 and November 1, the water supply to the power station was completely discontinued, which led to an increase in the water discharge in the river. It should be noted that in addition to water intake from the main channel of the Khodorzhiodara River to the power station, there is also a possibility of water intake to the irrigation canal, as can be seen in Figure 2.11, which should be taken into account in hydrometric measurements. Based on the results of measurements at a temporary gauging station, the dependence of water discharge on the water level in the river, shown in Figure 2.18, was determined for Khodorzhiodara River.
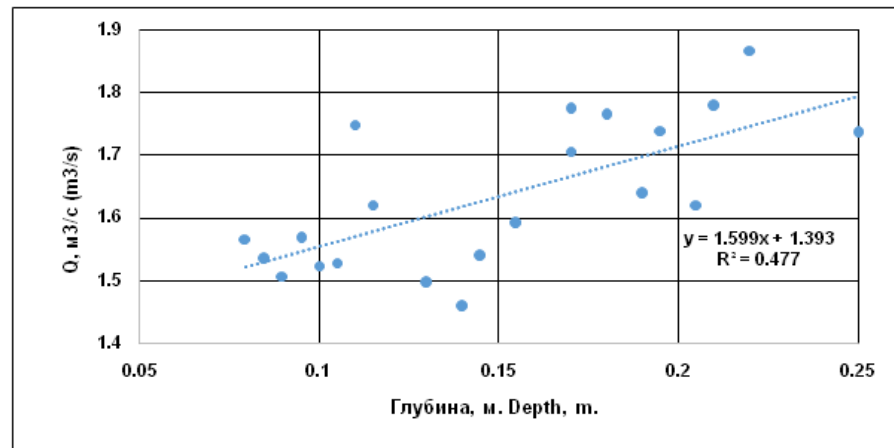
Fig. 2.18. Dependence of water discharge of the Khodorzhiodara River and corresponding change in the river's depth.

According to the graph in Fig. 2.18, the close relationship between parameters is low, with a correlation coefficient of r = 0.43 ± 0.12. The mean square error (δ) of the regression equation for y with respect to x is equal to δ y / x = 0.09, i.e. the deviation of points in percentage terms is 11.9% and is small.

In conclusion, we'd like note the following. As a result of field works in 2017, potential locations for the establishment of gauging stations and measurement of water discharge were identified for the Darzhomdara and Khodorzhiodara rivers. Water discharge measurements in the rivers were carried at using the float method. For the Khodorzhiodara River, the dependence of the water discharge on the water level in the river was determined based on the data obtained at the temporary gauging station, which can be refined during subsequent measurements.

In the future, in order to obtain long-term and more accurate data on the amount of water discharge and level on the Darzhomdara River, it is necessary to organize a gauging station, with the installation of a device measuring the change in the hydrostatic water pressure. It is recommended to install an acoustic device measuring the water level under the transport bridge on the Khodorzhiodara River, but in this case it is necessary to take into account water intake by the irrigation canal and power station.

3. Glaciological research.

In 2017, a reconnaissance survey of the No. 183 [4] glacier was carried out in the Darjomchdara River's basin (Fig. 3.1). As a result, the photographs of the glacier tongue's attributes were taken and the boundary of the open ice on the tongue was fixed with the GPS. It is established that the upper part of the firn area is located at an altitude of 5200 m. a.s.l., and the lower limit of open ice, at an altitude of 4158 ma.s.l.Part of the glacier, covered with moraine, descends to the elevation of 4085 ma.s.l. and extends down along the valley at 616 m, the thickness of the moraine reaches 10 cm. The modern moraine coating smoothly passes into the ancient moraine, which complicates the study of the glacier by remote methods. The elevation of the ancient moraine upper part is 3930.4 m a.s.l. Below, the bed of the valley descends downwards in the form of a terrace and has no traces of any previous glaciations.

Fig.3.1 View of the №183 glacier

2.2 The results of the analysis of published data, decoding of space images in 2016-17.

1.Meteorological research

An analysis of changes in climatic conditions in the area of interest was carried out on the basis of the data of the Tajik Hydro-Meteorological Service on the meteorological stations (MS) of Irht and Rushan. The Irht MS is located 55 km to the east (72.62^0 el, 38.170 nl) of the area of interest, at an altitude of 3276 m a.s.l., and the Rushan MS is 40 km to the west (71.55^0el, 37.95^0nl.), at an altitude of 1983 m a.s.l..

As can be seen in Fig.1.1, the average annual temperature of the surface air layer at these meteorological stations differs massively due to different altitudes above sea level. At the same time, synchronism of temperature changes is observed at both stations and is especially evident in the period from 2004 to 2016. During the observation period from 1991 to 2016, an increase in air temperature over a linear trend of about 1.5^0C for 25 years or with a gradient of 0.06°C/year is observed at both stations. A similar change in air temperature in the area of interest, taking into account its altitude, can be predicted for the next decade.
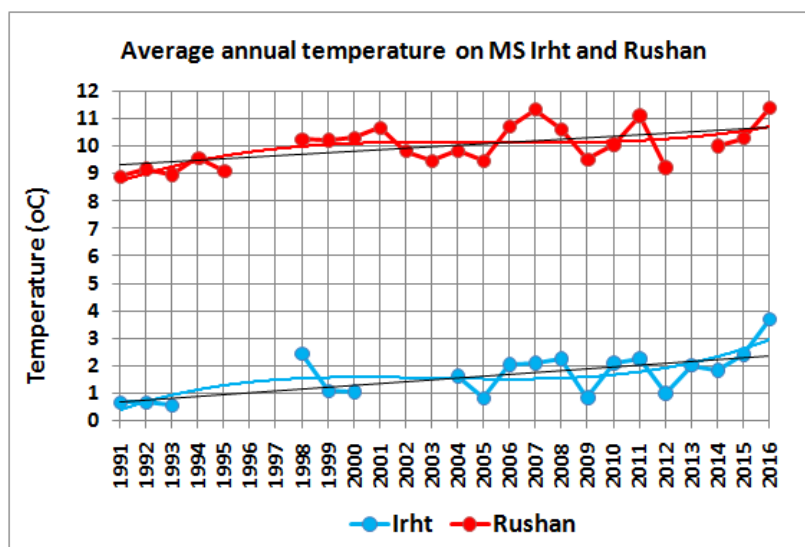
Fig. 1.1 Change in the average annual air temperature on the Irht and Rushan meteorological stations

The change in atmospheric precipitation from the Irht and Rushan meteorological stations is shown in Figure 1.2. Atmospheric precipitation during the observation period, as well as the air temperature, show signs of synchronous change in both stations, but there is no clear trend of change. The annual sum of atmospheric precipitation on the Irht meteorological station varies in the range 100-200 mm, on the Rushan MS - 200-400 mm. The amplitude of the oscillations of the atmospheric precipitation is about 100 mm in the first case and 200 mm in the second. In terms of the forecast, one can expect that a similar change in precipitation, taking into account the altitude, will be observed in the next decade in the area of interest. Given that the area of interest has a minimum altitude of about 2200 m, it can be assumed that the air temperature and precipitation parameters within it will be close to those of the Rushan station.
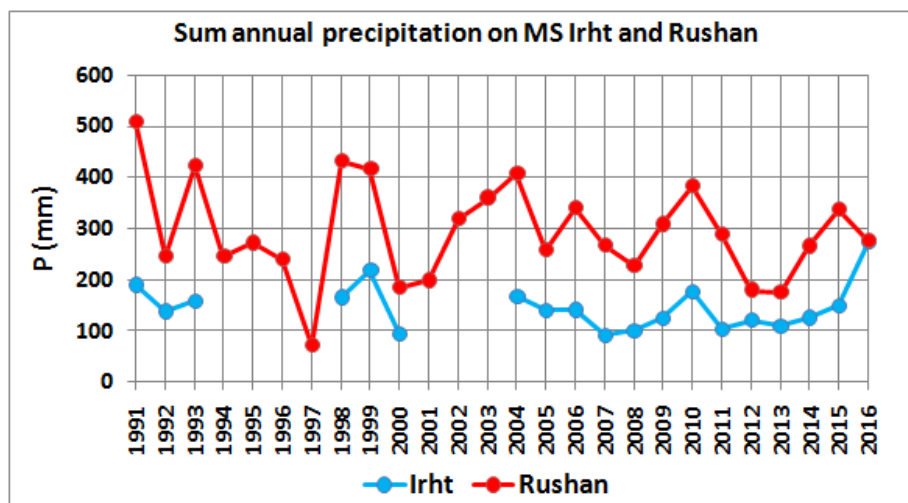
Fig. 1.2 Change of annual precipitation sums for the Irht and Rushan meteorological stations

As can be seen in Figures 1.1, 1.2, during the change in air temperature and atmospheric precipitation, an uneven periodicity of several years is observed, which can be used to forecast the change in these parameters at similar time intervals.

2. Glaciological research.

The purpose of this study was to determine the degree of glacier change over a multi-year period, in Tajikistan, in the Bartang River basin, in particular, in the Darjomch and Bartang villages. Space images of the "KH-4B" satellite, the "CORONA" satellite system, with a resolution of 1.8m (6 feet), the Declass 1 section (1996) and the "Landsat 8" satellites with a resolution of 15m were used to identify the glacier boundaries at different times. "Landsat 5" (TM) with a resolution of 30 m, obtained from the Internet service of the US Geological Agency (USGS), "Sentinel 2" with a resolution of 10 m, from the Internet service of the European Space Agency also were used as well as the images of the "WorldView 2", "Ikonos" satellites from the Internet service "Google Earth" with a resolution of 0.5 m, 1.0 m and topographic maps of scale 1: 100000.

The interpretation technique included the co-registration of space images obtained at different times, while the images of "Landsat 8" with the initial georeferencing with an accuracy of <30 m and ultra-high resolution images of "WorldView" with the original accuracy of the referencing up to 5m were used as the base image. When co-registering images that do not have original georeference ("Corona" images), the check points were chosen near the glacier's tongue,

on stable, relatively shallow relief. In this case, geometric distortions of the image are minimized due to the angle of survey and the inclination of the relief surface.

The minimum interpretation error for all used images corresponds to the resolution value of the image. For the interpretation results, the evaluation of the relative spatial positioning accuracy is of primary importance, which was performed by measuring the difference in the position of the boundaries of stable relief forms on the compared base image and another image and another kind of data georeferenced to the base image. The relative positioning error in our case has a maximum value of about several tens of meters.

In the area of Darjomch village, glaciers No. 783 and 780 were selected for study, according to the Glaciers Catalog of the USSR (GCU), Volume 14, Issue 3, Part 13 [4]. The first is located in the Darjomchdara River basin, and the second one - in the Chadegiv River basin (Fig. 2.1).

The No. 783 Glacier is a glacier of the valley type, with north and north-west orientation (according to the CGS). As of 1966-1971 (the period of the catalog compilation) it had a total length of 4 km, from which the open part, not covered by the moraine, was 3.2 km. Accordingly, the areas were as follows: total area - 2.1 km^2 and an open area - 1.9 km^2. The volume of the glacier was 0.0822 km^3 (Appendix 2). It should be noted that according to the information from the mentioned catalog in the period 1966-1971 there were no aerial images for the region, therefore, the boundaries of glaciers for this period have no justification. This reduces the reliability of the information given in the catalog on the observed glaciers.
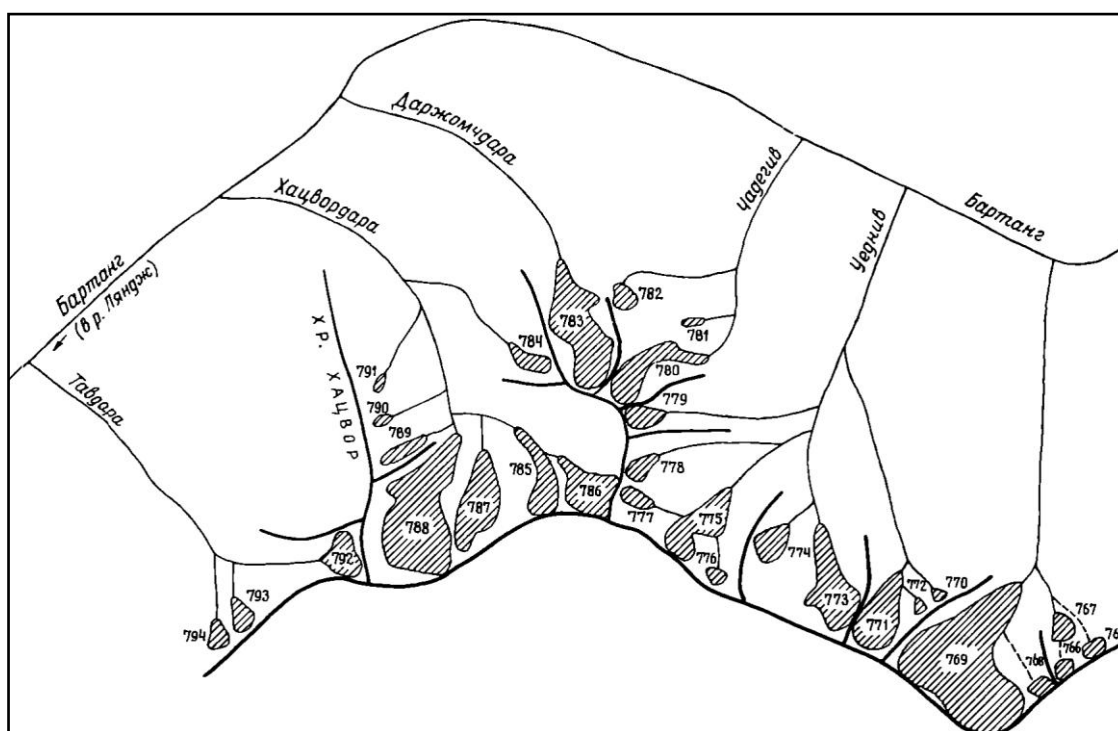
Fig.2.1 Scheme of the glaciers location in the basins of the rivers Uedniv, Chadegiv, Darjomchdara, Khatsvordara and Tavdara.

Space images of "KH-4B", the "CORONA" satellite system, dated 18/08/1968, with a resolution of 1.8m (6 feet), the section Declass 1 (1996) and "Landsat 8" with a resolution of 15 m, obtained from the Internet service of the USGS were used to detect the different-time positions of the boundaries of the No. 783 glacier as well as "WorldView 2" image with a resolution of

0.5m from the "Google Earth" and a topographic map with a scale of 1: 100000 with a reflection of the terrain condition for 1969-1984.

The boundary of the No. 783 glacier was obtained in 1968 from the "KH-4B" satellite image and is shown in Figure 2.2. At that time, the tongue of the glacier had a narrowed wedge shape, due to the prevailing recession of the eastern lateral boundary (this is a typical phenomenon due to more warming up by the sun of the eastern sides of the valleys after noon,), with an ice break at the end of the tongue (Fig.2.3).The total length of the glacier at this time, according to the results of our interpretation was 3900 m, the area - 1.92 km^2. This result is close to the parameters from the GCU for the period 1966-1971 on the total length of the glacier of about 4000 m and the area of 2.1 km^2. In this case, it is necessary to pay attention to the fact that according to the results of interpretation, in 1968 (Fig.2.2), over the entire length of the total length, the glacier was open, with the presence of a small median moraine area. This fact is an evidence of an underestimation of the length of the open part of the glacier in the GCU (3200m), probably due to the absence of aerial images of the glacier for the period 1966-1971.
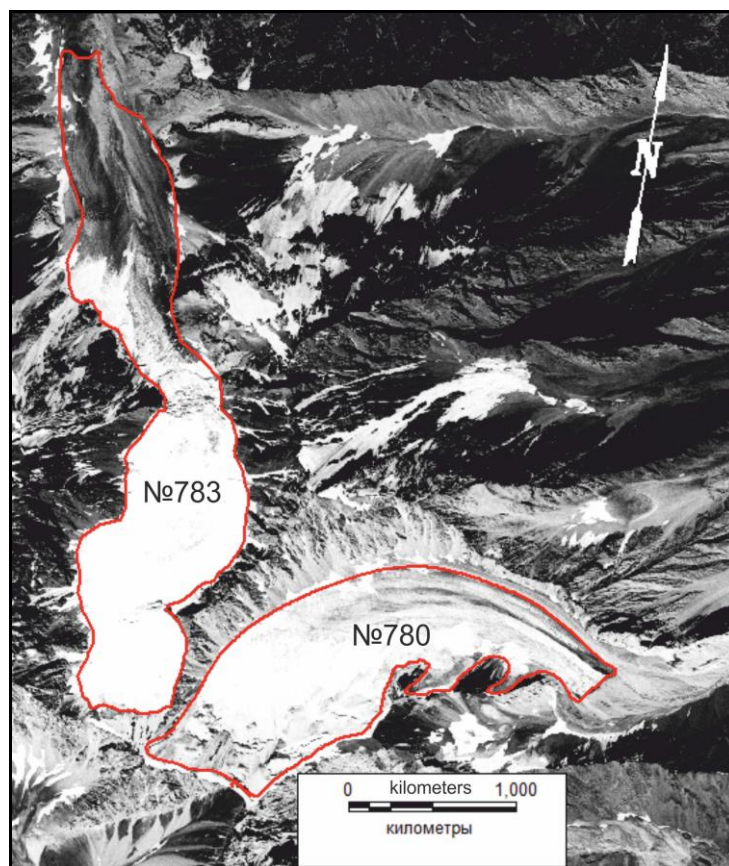
Fig.2.2 Borders of the №780 and №783 glaciers in 1968, according to the "KH-4B" image of the "Corona" system.
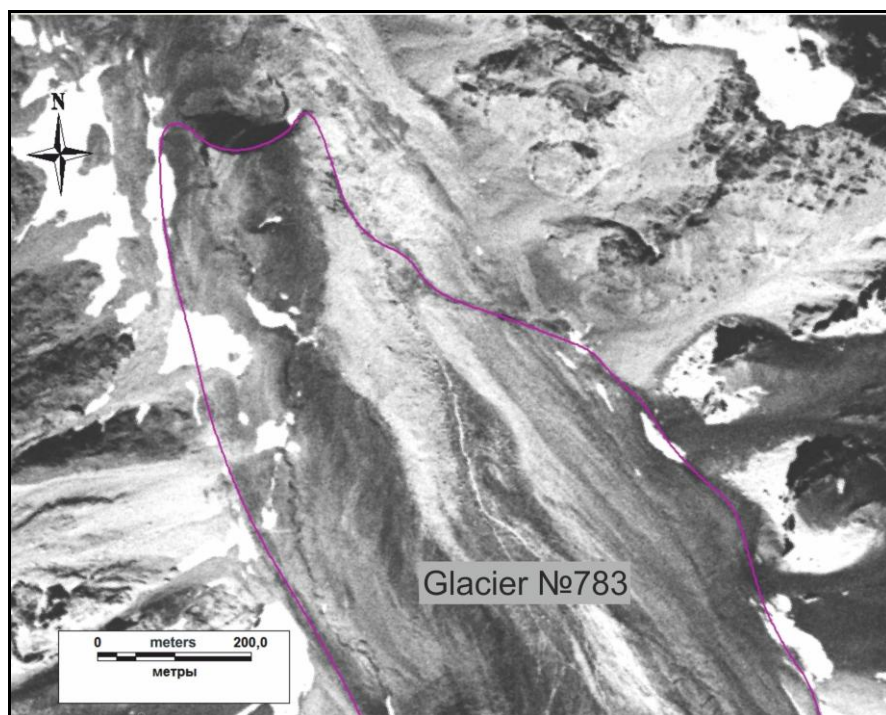
Fig.2.3 The border of the No. 783 glacier tongue in 1968, according to the "KH-4B" image of the "Corona" system.

On a topographic map with a scale of 1: 100000 (sheet J42-72 with the state of the terrain for 1969-1984, and a sheet J43-61 with the state of the terrain for 1975-79), the boundary of the glacier is shown in Figure 2.4. At this boundary, the length of the glacier is 3600 m. The total area of the glacier on the map is 1.45 km^2. Thus, in the period 1969-1984 it can be assumed that the length and the area of the glacier is reduced relative to 1968, but given the uncertainty of reflecting the situation on the terrain when mapping by the time and by the data used, this requires additional confirmation. According to the available data, it can be assumed that the map reflects the position of the boundary of the open part of the glacier for a time close to 1984. In this case, there is a fact of the tongue's recession by 300m from the position of 1968. In general, information about the boundary of the glacier on the topographic map has a great uncertainty about the accuracy of the definition of boundaries and their time, and therefore it can be used presumably only.
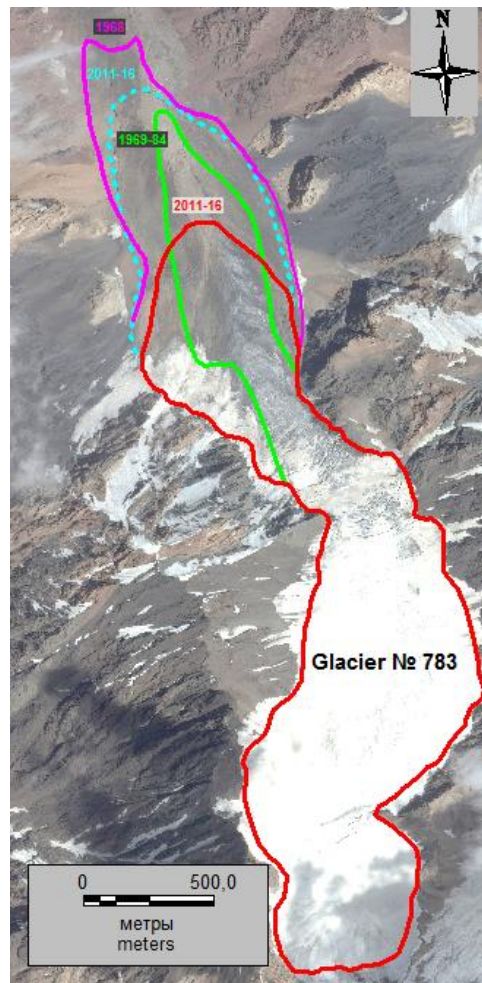
Fig. 2.4 Borders of the № 783 glacier by space images in 1968, 2011-16 and by the topographic map in 1969-84. (green color). The blue color indicates the supposed modern boundary of the glacier beneath the moraine cover. Red - a modern border on open ice and, partly, beneath the moraine. Background - "World View 2" image dated 12/08/2011.

The current state of the No. 783 glacier was studied by the "WorldView 2" images from 12/08/2011 and by the "Landsat 8" images from 20/09/2016. At this time, as seen in Figure 2.4, the glacier lacks a clearly expressed end of the tongue due to the immersion of part of the glacier under the moraine cover in the north-west direction. The boundaries of open ice on these satellite images practically coincide in 2011 and 2016 and the length of the common boundary of the open part of the glacier is 3150 m, and the total area of the glacier is about 1.53 km^2.In this case, the total area of the glacier includes not only the area of the open ice, but also a part of the morainic surface of the glacier, where there are clear signs of the presence of ice in the form of cracks. In this case, it should be noted that the area of the glacier of 1.53 km^2, along the border of 2011 and 2016, is larger than the glacier's area of 1.45 km^2 obtained from the map on the 1984 border, which is probably due to earlier performed topographic mapping of only the open ice of the glacier. In addition, attention is drawn to the fact that the length of the open part of the ice by the GCU for the period 1966-1971 is close to the length of the open part of the glacier for the period of 2011-16 that we determined. This fact, taking into account the reliability of the results of interpretation results of the "Corona" system space image from 1968, indicates that the length of the open ice by GCU for the period 1966-1971 is incorrect.

In addition to the obvious boundary of the No. 783 glacier on the open ice in 2011 and 2016, the current probable limit of ice spreading in the north-west direction under the moraine cover was

determined, which is shown in Figure 2.4 with a dashed blue line. In the extreme northern part, this boundary is drawn on the manifestation of thermokarst funnels, which usually indicate the presence of ice under the moraine cover (Fig. 2.5). This boundary is spatially, by the position of the tongue end, close to the 1984 boundary, obtained from the topographic map.
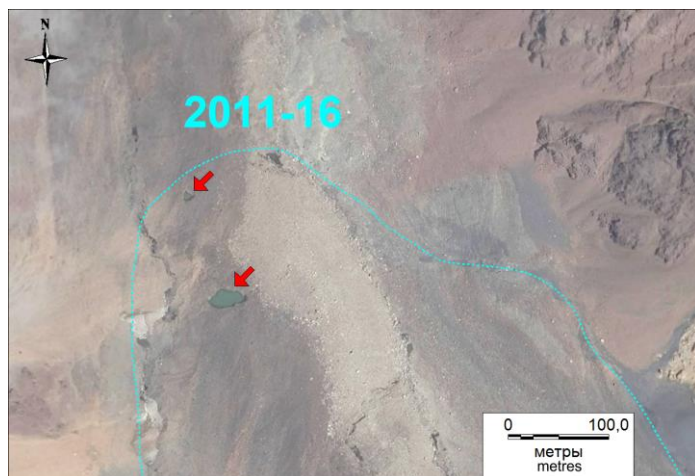
Fig. 2.5 The assumed boundary of the ice spreading under moraine cover for the period 2011-2016. Red arrows point to thermokarst funnels. Background - "WorldView 2" image from 12/08/2011.

Thus, the process of the No. 783 glacier degradation probably occurred from 1968 to 1984 in the form of an intensive recession of the glacier's tongue by 300 m, at a speed of about 18.8 m/year. At the same time, at the end of this period, the degradation rate began to slow down, the moraine covered the tongue, and the length and the area of the open part of the glacier reduced to the state currently observed. As a result, a significant part of the glacier was preserved under the moraine cover, while the rate of melting of ice covered with solid moraine was significantly reduced due to the thermal insulating property of the moraine. The decrease in the volume of ice under the moraine occurred mainly due to a decrease in the thickness of the ice. The boundary of this ice spreading, as mentioned above, is shown in dotted lines, and the total area of the glacier along this boundary is 1.83 km^2. This boundary is accepted as modern as of 2016, and the change in the area of the glacier since 1968, which is represented by a decrease of 0.09 km^2 or 4.7%, is determined relative to it (Table 2.1).

Changing in the area of the № 783 glacier   Table 2.1

Year of the boundary	Glacier's area (km^2)	Glacier's area change (km^2)	Time period (years)	Rate of glacier's area change (km^2/year)
1968	1,92			
2016	1.83	0.09	48	0.0019
1968-2016		0.09(4,7%)		

In general, the overlap of the glacier in its lower part by moraine cover and gradual recession of the open ice boundary to feeding area with increasing of the area covered by moraine will remain with the warming up trend. In this case, the assessment of the change in the length and the area of the glacier is difficult due to impossibility to determine precisely the boundary of the ice distribution beneath the moraine cover. The high degree of tongue coverage by the moraine on

the No. 783 glacier and the absence after 1968 of a clear boundary of the tongue makes it difficult to compare the different boundaries based on the interpretation results of space images even with ultrahigh resolution. For this reason, for a more accurate determination of the rate of degradation of glaciers in the investigated region, the No. 780 glacier was studied. This glacier is located east of the No. 783 glacier, in the Chadegiv River basin. The basins of both glaciers have a partially shared watershed (Figure 2.2). The advantage of the glacier №780 is the presence of only a slight surface moraine and a clear boundary of the tongue.

The valley glacier No. 780, according to the Catalog of Glaciers of the USSR [4] (Figure 2.1), has a northeastern and eastern orientation and as of 1966-1971 its total length was 3 km and the area was 1.7 km2. The volume was estimated at 0.0598 km3.

The boundary of this glacier and, in particular, its tongue, as the most variable part, for 1968 was obtained by interpreting the mentioned "KH-4B" space image, dated 18/08/1968 (Fig 2.2, 2.6). At this time, the length of the glacier was 2610 m, and the area was 1.548 km^2 (Table 2.2). In this case, attention is drawn to a significant difference in the determination of the glacier length from the GCU and from the satellite image, even though the determination time in both cases practically coincides. This contradiction may be due either to the definition of glacier parameters in the GCU from data much earlier than the time of compiling this GCU, or due to a lack of information, in particular, the absence of aerial images mentioned above.

The boundary of the №780 glacier in 1975-1979 was obtained from a topographic map with a scale of 1: 100,000, which reflects the state of the terrain for 1975-1979. On this boundary, the glacier tongue recession is observed from 1968 to 1979, in average by 50 - 60 m, and in the extreme north-eastern part of the tongue by 120 m with a simultaneous decrease in the area (see Tab.2.2).
The boundary of the same glacier in 1992 was determined from the "Landsat 5" (TM) satellite image with a resolution of 30 m, dated 27.09.1992. By this time, the northeastern part of the tongue recessed to the greatest extent by 100 m, with a slight recession of the southeastern part, and during the same period of 1979 - 1992, the width of the glacier with a recession of the northern lateral boundary by 40- 70 m (see Fig. 2.6).The total area of the glacier due to this significantly decreased.

Based on the result of the "Ikonos" satellite image interpretation from 12/10/2007, with a spatial resolution of 1.0 m, the boundary of the №780 glacier was determined in 2007. This space image is used as the background in Figure 2.6. This figure shows that the recession of the glacier continued, but, to a greater extent, the south-eastern part of the tongue recessed in average by 40 m, with a corresponding decrease in the total area of the glacier.

The boundaries of the glacier's tongue in 2014 and 2016 were obtained from the interpretation results of the "Landsat 8'"satellite images from September 15, 2014 and September 20, 2016, from the USGS service. These results confirm the continuation of the trend of the glacier tongue recession and its area reduction.
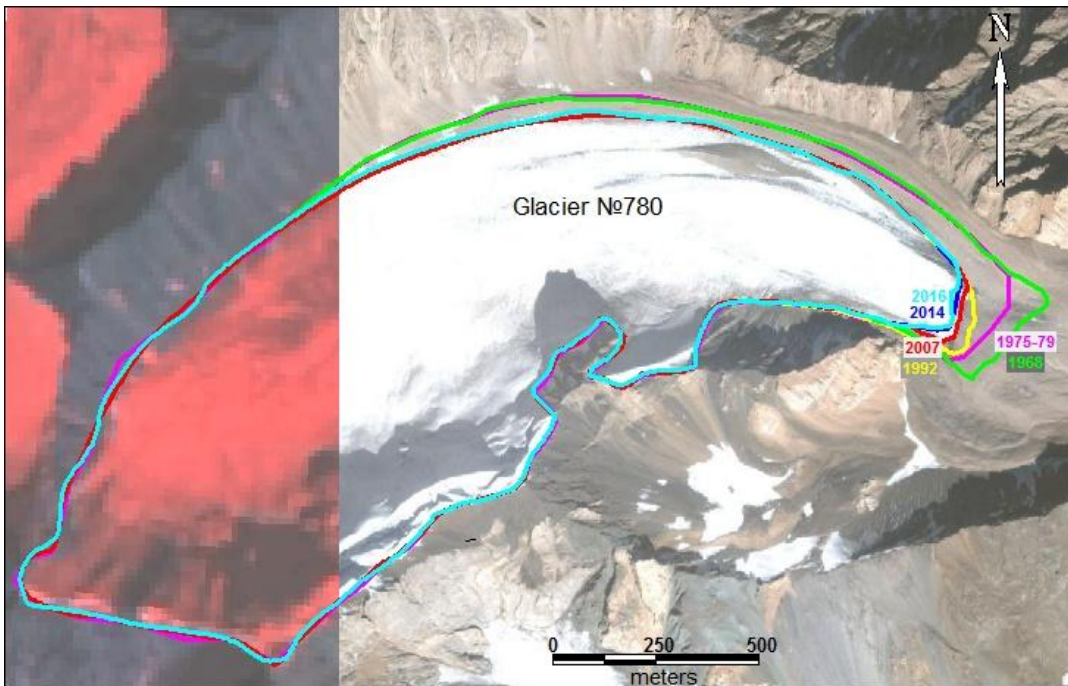
Fig. 2.6 The boundaries of the No. 780 glacier in different years. Background - "Ikonos" space image from 12/10/2007.

Change in the № 780glacier area   Table 2.2.

Year of boundary location	Glacier's area (km^2)	Area's change(km^2)	Period of time (years)	Rate of area's change $(km^2/year)$
1968	1,548			
1975-**1979**	1.531	0.017	11	0.0015
1992	1.436	0.095	13	0.0073
2007	1.428	0.008	15	0.00053
2014	1.424	0.004	7	0.00057
2016	1.423	0.001	2	0.0005
1968-2016		0.125 (8.07%)		
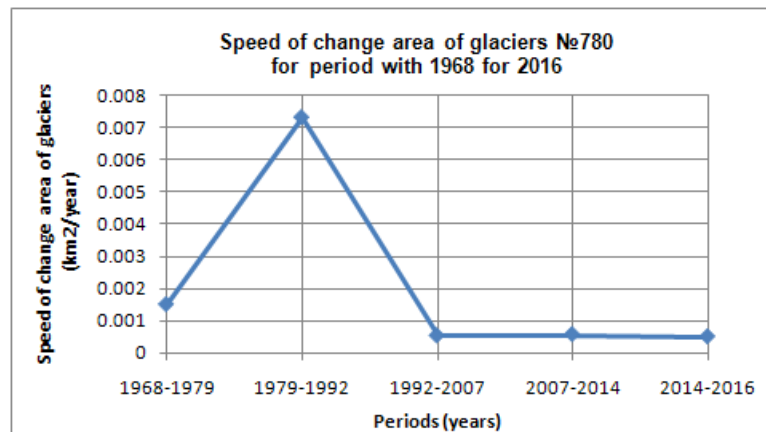
Fig. 2.7 Rate of change in the No. 780 glacier area from 1968 to 2016

In general, from 1968 to 2016, the area of the No. 780 glacier decreased by 0.125 km^2 or by 8.07%, while the length of the glacier along the center line decreased by 160 m from 2580 m to 2420 m, and the front part of the tongue recessed in average by 175 m from 120 m to 230 m. A feature of the area reduction of this glacier is the significant recession of its northern lateral boundary by 40 -75 m in the period from 1975-1979 until 1992. This is due to the southern exposure of the northern edge of the glacial valley, which provides a local increase in the temperature of the surface and air. As can be seen in Table 2.2, the rate of change in the glaciers area was greatest in 1970s and 1980s (Figure 2.7), and then it dropped significantly. In general, such an order of velocities is common for glaciers of the Tien-Shan and Pamirs. In general, it can be noted that at the site of interest in the basins of the Khadorzhviodara, Darjomchdara, Hatsvordara, Uedniv and Tavdara rivers, the glaciers have a predominant northeastern and northwestern orientation, which contributes to their relatively less degradation in the warming up conditions.

With respect to glacier runoff, according to the two glaciers considered above, it can be assumed that its value on the No. 783 glacier will decrease as its part, covered by moraine, increases, until it reaches the minimum limit characteristic for rock streams. At the same time, glacier runoff will be relatively stable on the No. 780 glacier, which mainly depends on the change in the average summer air temperatures. Concerning the size of the water reserves concentrated in these glaciers and corresponding to the volume of ice and the equivalent volume of water, it can be asserted that for the period 1968-2016, they decreased in proportion to the decrease in the area by approximately 5% (№783) and 8% (№780).

In addition to the glaciers considered above, a group of glaciers in the basin of the Khadorzhviodara River was studied. They are glaciers No. 18-22 by the Catalog of Glaciers of the USSR. Volume 14. Issue 3. Part 13 [4] (Fig. 2.8, 2.9).
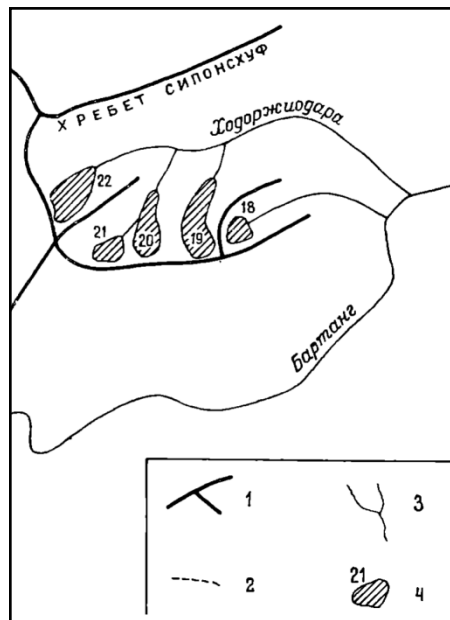
Fig. 2.8. Scheme of glaciers location in the basin of the river Khadorzhviodara River.
1 - watershed. 2 - iceshed. 3 - river. 4 - glacier and its number
in the Catalog of Glaciers of the USSR.

The location of the No. 18, 19, 19a, 20 glaciers boundaries in 1968 was determined from the "KH-4B" satellite image of the "CORONA' satellite system from 18/08/1968, with a resolution

of 1.8 m (6 feet) and is shown in Figure 2.10; the area values are given in Table 2.3. The boundaries of glaciers in 2002, 2011, 2016 were obtained by interpreting the satellite images: the "Ikonos" from 10.10.2002 and from 24.07.2011, with a resolution of 1 m and the "Sentinel 2" images from August 22, 2016 with a resolution of 10 m. Figures 2.11, 2.12 show the boundaries of the glaciers in 1968, 2002, 2011, 2016 on the background of "Ikonos" images from 2002 and 2011 respectively.

The glaciers areas in different years are defined in the GIS MapInfo and are shown in Table 2.3. The same table shows the rates of change in the area of glaciers. As follows from Table 2.3, all the glaciers considered over a long time interval have a general tendency to reduce the area. Short-term periods of stabilization and a slight increase in area are also observed. But as for boundaries of glaciers during these periods, the influence of interpretation errors, which are close to the values of the area change, is possible. In general, the range of rates of decrease in the area of the glaciers is from 0.00017 to 0.0026 km^2/year. The change in these rates from the beginning to the end of the observation period does not show a trend of their significant increase in a final period of time (Figure 2.13). The reduction in the area according to the most reliable results of the analysis of changes in glaciers No. 19 and 19a is 5.9 - 8.9% over a period of 48 years from 1968 to 2016, that is, the average gradient of the change is 0.12-0.19%/year. The maximum decrease in the area was recorded on the No. 20 glacier - 20.7% with a gradient of 0.4%/year. Since the volume of glaciers depends on their area, we can approximately assume that its decrease corresponds to the indicated reduction in area.
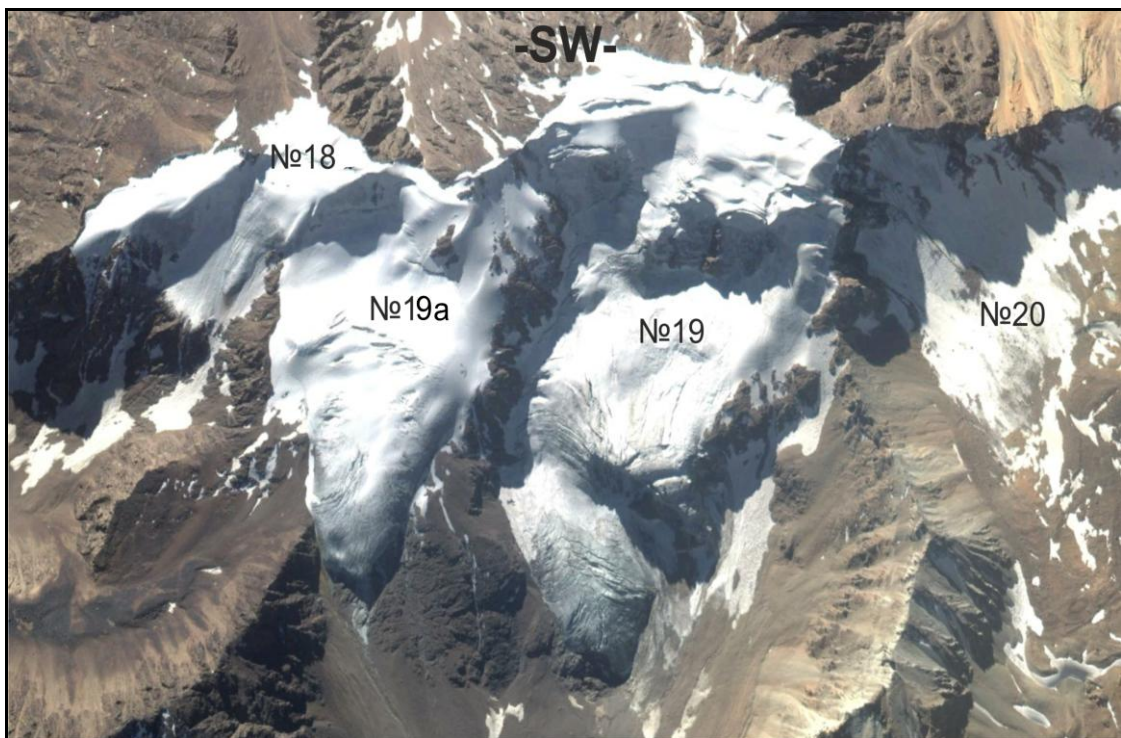
Fig. 2.9 View of the No. 18, 19, 19a and 20 glaciers in 2002
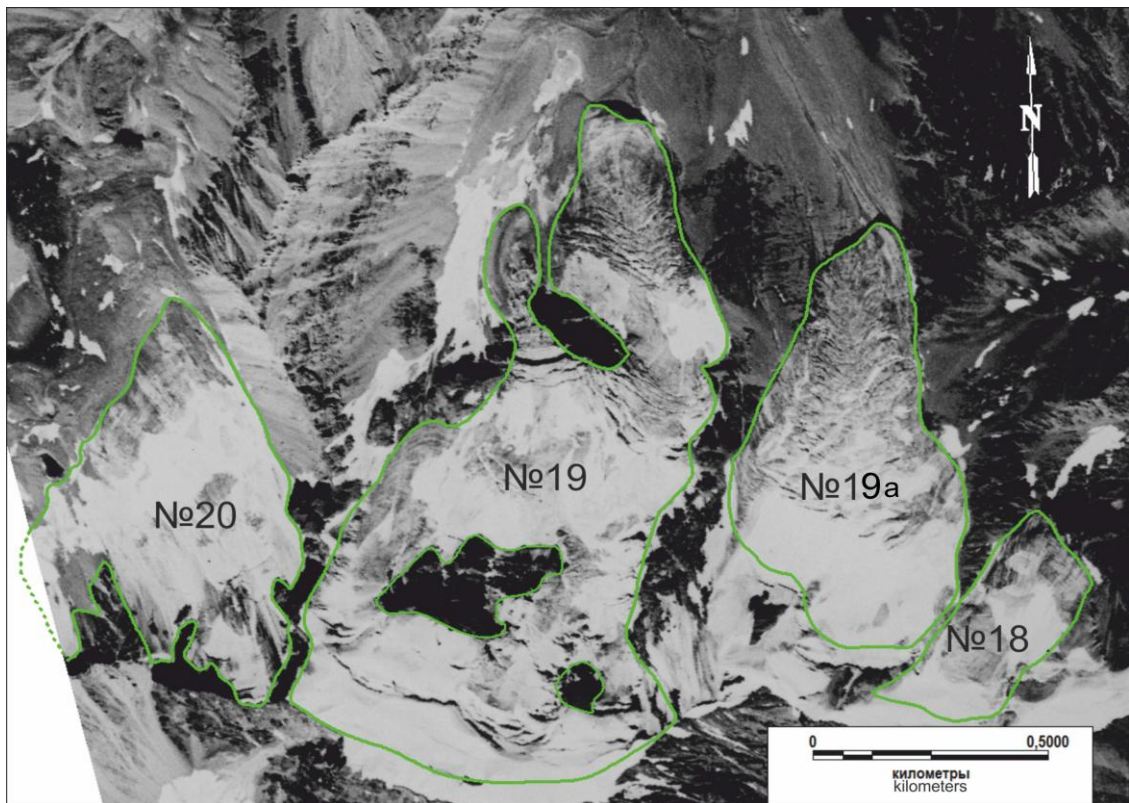
Fig. 2.10 Location of the №18, 19,19a, 20 glaciers boundaries in 1968 by the "KH-4B" satellite image, "CORONA", from 18/08/1968.
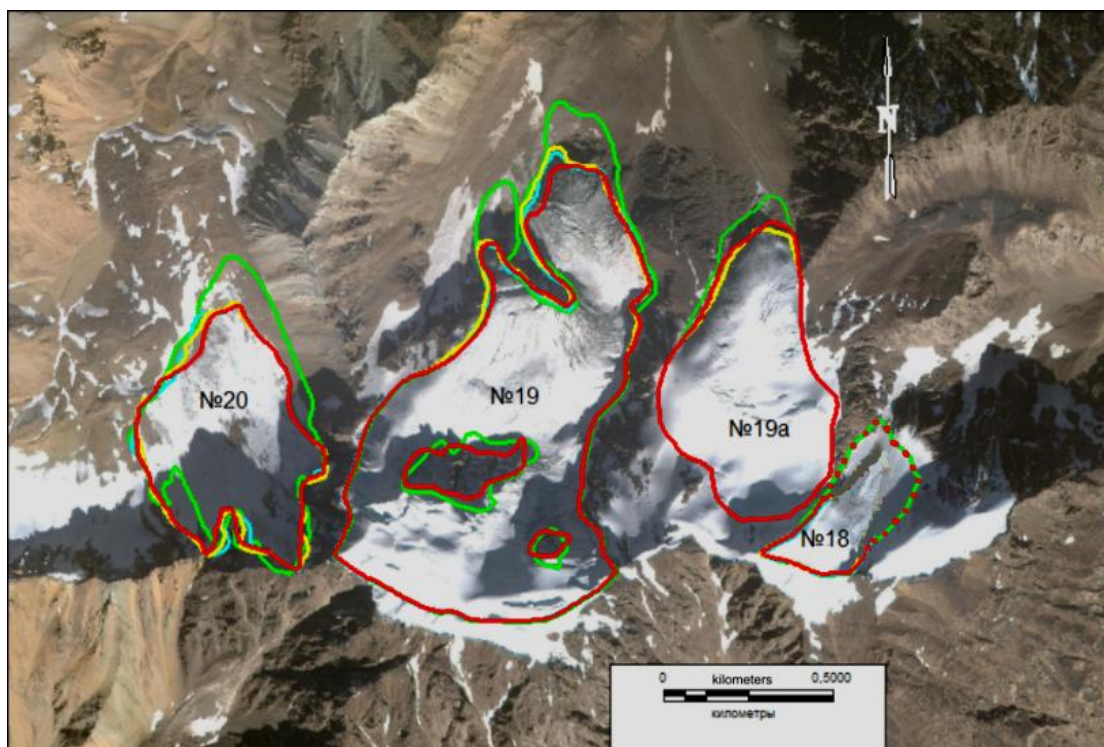
Fig. 2.11 Boundaries of the №18,19, 19a, 20 glaciers in 1968 (green), 2002 (yellow), 2011 (blue) and 2016 (red) years on the background of "Ikonos" image from 10.10.2002.
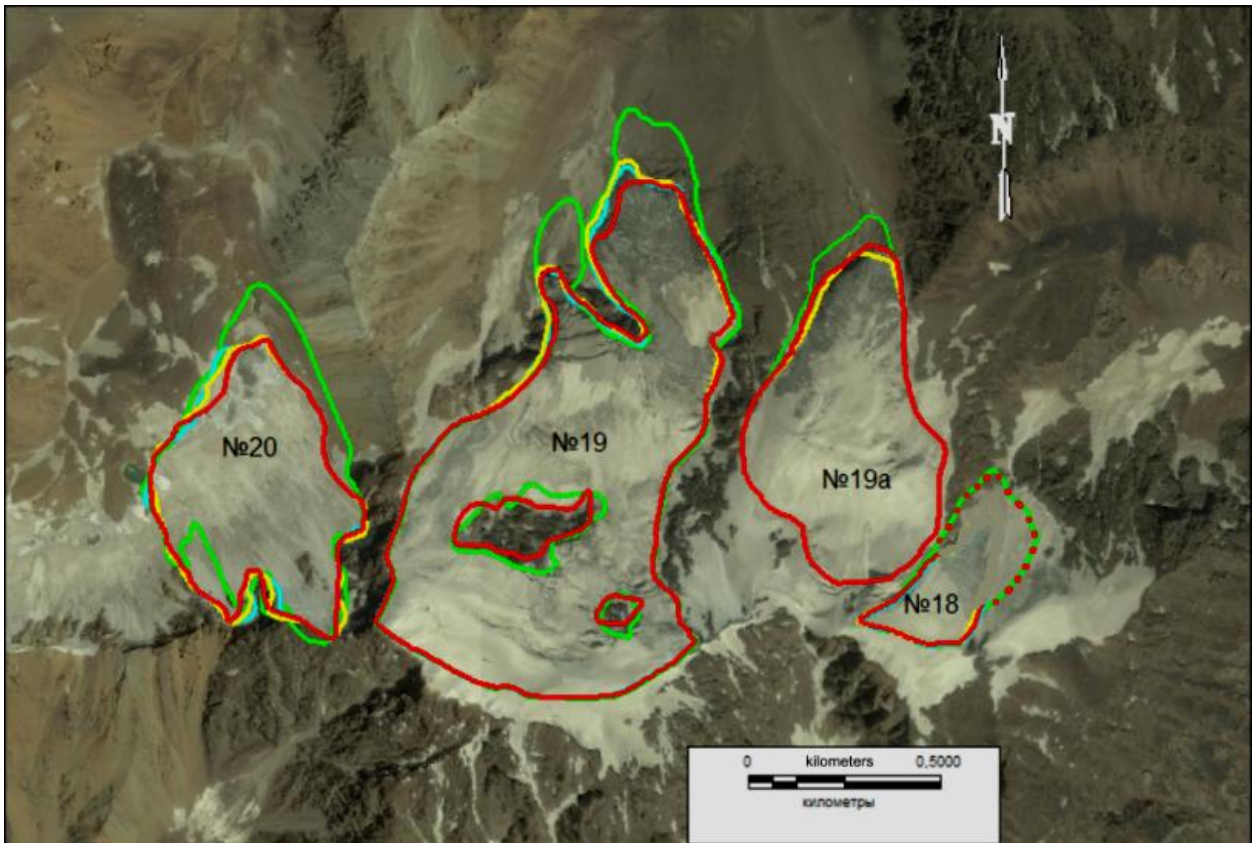
Fig. 2.12 The boundaries of the №18.19, 19a and 20 glaciers in 1968 (green), 2002 (yellow), 2011 (blue) and 2016 (red) on the background of "Ikonos" image from 24.07.2011.

Table2.3

Glacer's№	Year of boundary location	Glacier's area (km^2)	Change of glacier's area (km^2)	Period of time (years)	Rate of glacier's area change (km^2/year)
18	1968	0.0947			
	2002	-«-	0.0	34	0.0
	2011	-«-	0.0	9	0.0
	2016	-«-	0.0	5	0.0
	1968 - 2016		0.0		
19a	1968	0.31098			
	2002	0.2881	- 0.0229	34	-0.00067
	2011	0.2927	+ 0.0046	9	+0.0005
	2016	0.2927	0.0	5	0.0
	1968 - 2016		-0.0183 (5.9%)		
19	1968	0.7109			
	2002	0.6572	- 0.0537	34	-0.0016
	2011	0.6538	-0.0034	9	-0.00037
	2016	0.6409	-0.0129	5	-0.0026
	1968 - 2016		-0.07 (9.8%)		
20	1968	0.30198			
	2002	0.2499	-0.0521	34	-0.0015
	2011	0.2483	-0.0016	9	-0.00017
	2016	0.2396	-0.0087	5	-0.0017
	1968 - 2016		-0.0624 (20.7%)		
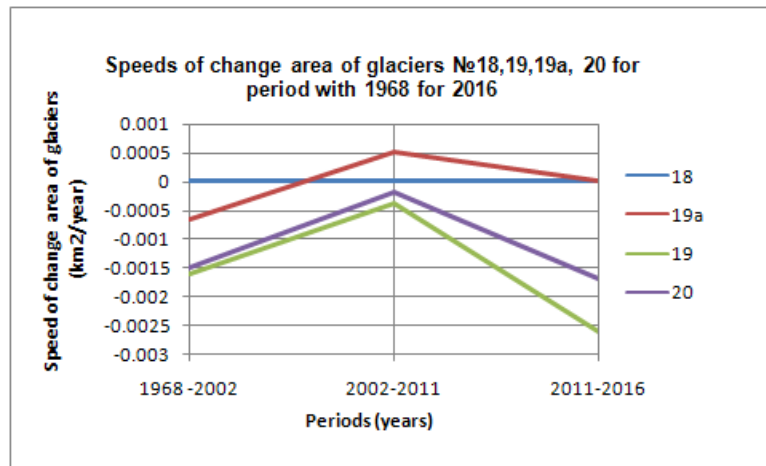
Fig. 2.13 Rate of change in the No. 18,19,19a and 20 glaciers area from 1968 to 2016

The linear recession of the tongues ends is uneven in different parts of the tongues, the maximum values are in the range of 70-180 m. The minimum decoding error for the "Sentinel 2" images is 10 m, for the "Ikonos" images - 1 m. The maximum decoding error is about several tens of meters for objects with fuzzy boundaries.

It is necessary to note the following points that were identified in the process of interpretation of the glaciers. Thus, No. 18 glacier due to its relatively high location, in accordance with the corrial morphological type (the end of the tongue is located at 4350-4370 m a.s.l.) was covered by firn field in the tongue part at the time of the space survey in 2002, 2011 and 2016, as it is seen in Figures 2.11, 2.12 and 2.14. Moreover, this situation was also observed in August 2016, so it is most likely that its area has not decreased since 1968, which is reflected in Table 2.3 in Figures 2.11, 2.12 and 2.13.
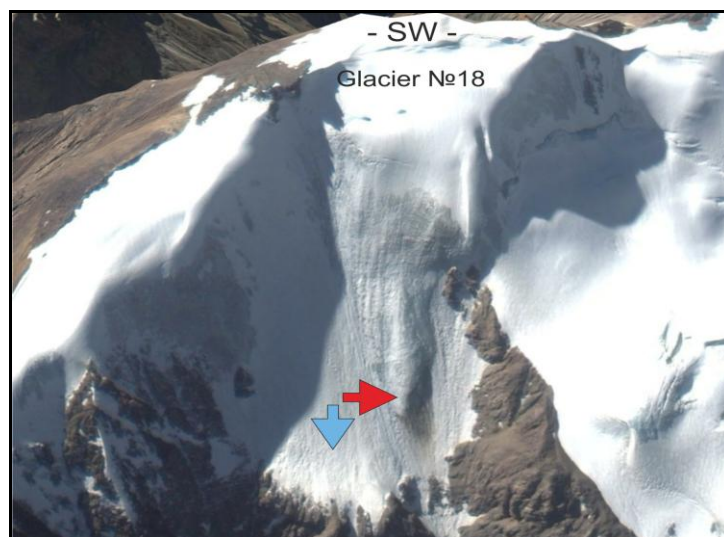
Fig. 2.14 №18 glacier, view in 2002. A blue arrow is a firn field covering the glacier's tongue, a red arrow is an ice brow on the glacier's tongue.

The No.19 glacier by the GCU as shown by the analysis of space images from 1968, 2002, 2011 and 2016, is actually represented by two glaciers, which we designated as No.19 and No.19a, are separated by a rocky crest with open ice tongues and a runoff in the north. Thus, the No.19 glacier on the scheme in the GCU (Figure 2.8) is shown incorrectly, in fact it consists of two glaciers. This may be due to the use of the results of topographical mapping in the compilation of the layout of the glacier in the GCU, according to which, as can be seen in Figure 2.15, glaciers

45

No.18 and 19 are not separated. At the same time, the No. 18 glacier basin in the presence of a clear rocky watershed with theNo.19 glacier has a common orientation and runoff in the east, that is, it cannot be united with the No.19 glacier, which has a runoff in the north.

Glaciers No.20, 21 and 22 do not have clear boundaries of tongues represented by open ice. The tongues of these glaciers are submerged under the moraine and are blocked by the latter, and open ice is observed in the area of glacier accumulation. One of the exceptions to this type of glacier is the No.20 glacier, whose tongue's boundary in 2002, 2011 and 2016 is partially traced against the background of the firn cover. In our case, a part of this glacier on the 1968 space image, is interpreted.

As can be seen in Figure 2.15, the boundaries of glaciers by a topographic map with a scale of 1:100000 (Sheet J42-72) with the state of the terrain for 1969-84 include significant parts represented by morainic sediments under which the presence of ice body of the glacier was assumed by the cracks and other signs of ice movement. This led to high estimates of the glaciers area at the time of mapping and, accordingly, the values of glacier areas included in the GCU. As noted in the GCU [4]: "*main information about the glaciers is obtained from large-scale maps, images of glaciers were refined by aerial images in 1966, so the information on the glaciers refer to this year. The allocation of the area of ice covered by moraine was carried out by the aerial images data, by the signs of ice movement forming morphologically integral whole with the glacier. The glaciers of the lower part of the Bartang River valley, on which there no aerial images, were not recorded in 1966, and were interpreted by on-ground visits and aerial survey conducted in September 1971*".Given this information, the glacier data from the GCU, Appendix 2, should not be used for comparison with the parameters obtained during the interpretation of space images without appropriate correction, as they are overestimated. For this reason, in this analysis, parameters from the GCU are not used directly to assess the changes in glaciers.
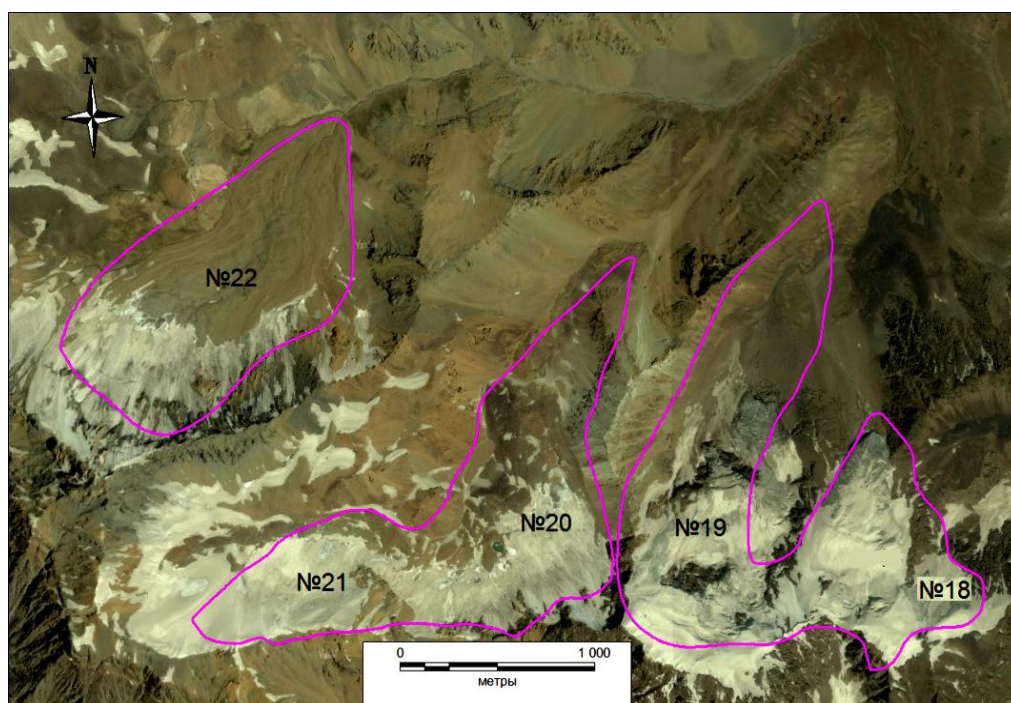
Fig. 2.15 The boundaries of the No. 18-22 glaciers by a topographic map of scale 1:100000 (Sheet J42-72) with the reflection of the terrain condition for 1969-84. Background −"Ikonos" image from 24.07.2011.

Thus, the analysis of changes in glaciers in the Bartang River basin showed a reduction in their area between 1968 and 2016 from 5% to a maximum of 21% with variation depending on the specific conditions of the functioning of glaciers. The water reserve concentrated in the glaciers considered, decreased accordingly.

Reference

1. Atlas of the Kyrgyz SSR. GUGK. M., 1987. p.86.

2. Bykov V.D., Vasiliev A.V. Hydrometry. - L : Gidrometeoizdat, 4th ed. 1977. - 448 p.

3. Catalog of glaciers of the USSR, Volume 14, Central Asia, Issue 1, Syr Darya. Part 6. The basin of the river. At-Bashi. L. 1974 - pp. 3 - 47.

4. Catalog of glaciers of the USSR, Volume 14, Central Asia, Issue 3, Amu Darya. Part 13. The Bartang basin. L. 1978 , p 106

Appendix 1

AutomaticMeteorologicalStation'sspecifications.

Anemometer:

OperatingTemperatureRange	-50° to +60°C (assuming non-riming conditions)
MountingPipeDescription	34 mm (1.34 in.) OD Standard 1.0-in. IPS schedule 40
MainHousingDiameter	5 cm (2.0 in.)
PropellerDiameter	18 cm (7.1 in.)
OverallHeight	40 cm (15.7 in.)
OverallLength	57 cm (22.4 in.)

Weight	1.0 kg (2.2 lb)

Windspeed

Range	0 to 100 m/s (0 to 224 mph)
Accuracy	±0.3 m/s (0.6 mph) or 1% of reading
StartingThreshold	1.0 m/s (2.2 mph)
DistanceConstant	2.7 m (8.9 ft) 63% recovery
Output	ac voltage (three pulses per revolution) 90 Hz (1800 rpm) = 8.8 m/s (19.7 mph)
Resolution	$(0.0980$ m $s^{-1})$/(scan rate in seconds) or $(0.2192$ mph)/(scan rate seconds)

Direction of the wind

MechanicalRange	0 to 360°
ElectricalRange	355° (5° open) electrical
Accuracy	±3°
StartingThreshold	1.0 m/s (2.2 mph) at 10° displacement
DistanceConstant	1.3 m (4.3 ft) 50% recovery
DampedNaturalWavelength	7.4 m (24.3 ft)
UndampedNaturalWavelength	7.2 m (23.6 ft)
Output	Analog dc voltage from potentiometer (resistance 10 kohm) Linearityis 0.25%. Life expectancy is 50 million revolutions.
Voltage	Power switched excitation voltage supplied by datalogger
DampingRatio	0.25

Precipitation gauge:

SensorType	Tipping bucket with magnetic reed switch (normally open)
Accuracy	2% up to 25 mm h^{-1} (1 in. h^{-1})

	3% up to 50 mm h^{-1} (2 in. h^{-1})
Resolution	0.1 mm (0.004 in.)
TemperatureRange	-20° to +50°C (heated)
HumidityRange	0 to 100%
Power	18 W @ 24 Vac (for heater only)
HeaterThermostatSetPoint	10°C ±3°C
ContactRating	24 Vac/dc (400 mAmaximum)
Mounting	Standard 1 in. pipe size, 34 mm (1.34 in.) diameter
CatchmentArea	200 cm^2 (31 in.^{2})
OrificeDiameter	16 cm (6.3 in.)
Diameter	18.5 cm (7.3 in.)
Height	30 cm (11.8 in.)
PowerPlugWeight	0.43 kg (0.95 lb)
Weight	1.16 kg (2.55 lb)

Air temperature sensor:

ElectromagneticCompatibility	Complies with EMC standard EN61326-1 Electromagnetic
Filter	Sintered PTFE
HousingMaterial	PC
HousingClassification	IP66
VoltageOutput	0 to 1 Vdc
AverageCurrentConsumption	≤ 3 mA (analogoutputmode)
OperatingVoltage	7 to 28 Vdc
SettlingTime	2 s (atpowerup)
TipDiameter	1.2 cm (0.5 in.)
Length	27.9 cm (11 in.)
HeadHeight	4 cm (1.6 in.)

BodyHeight	2.4 cm (0.9 in.)
BodyWidth	2.0 cm (0.8 in.)

Relative humidity sensor:

Sensor	HUMICAP 180R
MeasurementRange	0.8 to 100% RH (non-condensing)
ResponseTime	The response time for the RH specification is for the HUMICAP 180R at 20°C in still air with sintered PTFE filter and a 0 to 75% RH step change. 20 s (63% stepchange) 60 s (90% stepchange)
FactoryCalibrationUncertainty	The factory calibration uncertainty is defined as ±2 standard deviation limits. Uncertainty is at +20°C. Small variations are possible; see also the calibration certificate. ±0.6% RH 0 to 40% RH ±1.0% RH 40 to 97% RH

Appendix 2. Glaciers parameters in the Catalog of Glaciers of the USSR, Volume 14, Issue 3, Part 13

Glacier's №. in GCUS	Morphological type	General exposition	Glacier's length km	Open part km	Total area km^2	Open part area km^2	Height of firn line m	Ablation area km^2	Ablation of open part km^2	Glacier volume km^3
18	Corrial	NE	0.8	0.8	0.5	0.5	4620	0.2	0.2	0.0095
19	Valley	N.NE	2.4	2.4	1.2	1.2	4270	0.6	0.6	0.0355
20	Corrial-Valley	N.NE	2.0	2.0	1.0	1.0	4200	0.5	0.5	0.0270
21	Corrial	NE	0.8	0.8	0.4	0.4	4500	0.2	0.2	0.0068
22	Corrial-Valley	NE	1.9	1.9	1.2	1.2	4330	0.7	0.7	0.1048

Glacier's №.in GCUS	Morphological type	General exposition	Glacier's length km	Open part km	Total area km^2	Open part area km^2	Height of firn line m	Ablation area km^2	Ablation of open part km^2	Glacier volume km^3
780	Valley	NE.E	3.0	3.0	1.7	1.7	4620	0.9	0.2	0.0598
783	Valley	N. NW	4.0	3.2	2.1	1.9	4600	0.9	0.7	0.0822